Cationic Metallocene Polymerization Catalysts Based on Tetrakis(pentafluorophenyl)borate and Its Derivatives. Probing the Limits of Anion "Noncoordination" via a Synthetic, Solution Dynamic, Structural, and Catalytic Olefin Polymerization Study

Li Jia, Xinmin Yang, Charlotte L. Stern, and Tobin J. Marks*

Department of Chemistry, Northwestern University, 2145 Sheridan Road, Evanston, Illinois 60208-3113

Received October 18, 1996[⊗]

The synthesis and properties of two soluble, weakly coordinating derivatives of the tetrakis(perfluoroaryl)borate anion $B(4\text{-}C_6F_4TBS)_4^-$ and $B(4\text{-}C_6F_4TIPS)_4^-$ (TBS = *tert*-butyldimethylsilyl and TIPS = triisopropylsilyl) are reported. Reaction of the trityl salts of the above anions with a variety of zirconium and thorium L_2MMe_2 complexes in benzene or toluene affords the cationic ion-paired methyl complexes $L_2MMe^+X^-$ or the corresponding hydrido complexes $L_2MH^+X^-$ (L_2 = bis(cyclopentadienyl)- or cyclopentadienylamido-type ligand) when the reaction is carried out under dihydrogen. The solid state structure of the complex $(Me_5Cp)_2ThMe^+B(C_6F_5)_4^-$ has been characterized by X-ray diffraction. The $B(C_6F_5)_4^-$-based zirconocenium methyl complexes L_2MMe^+ are unstable at room temperature with respect to, among other factors, intramolecular C−H activation of the ligand framework. In general, the thermal stabilities of the $B(C_6F_4TBS)_4^-$- and $B(C_6F_4TIPS)_4^-$-derived complexes are greater than those of the corresponding $B(C_6F_5)_4^-$- and $MeB(C_6F_5)_3^-$-derived analogues. The relative coordinative tendencies of $MeB(C_6F_5)_3^-$, $B(C_6F_5)_4^-$, $B(C_6F_4TBS)_4^-$, and $B(C_6F_4TIPS)_4^-$ are estimated from the solution spectroscopic information and the structural dynamics of the ion-pairs and follow the order $MeB(C_6F_5)_3^- > B(C_6F_4TBS)_4^- \approx B(C_6F_4TIPS)_4^- > B(C_6F_5)_4^-$. The coordination of the neutral metallocene precursors to the cationic metallocenes is found to compete with counteranion coordination. Arene solvent coordination to the zirconium constrained geometry cation $[(Me_4Cp)SiMe_2(N^tBu)]ZrMe^+$ is also observed when $B(C_6F_5)_4^-$ is the counteranion. $(1,2\text{-}Me_2Cp)_2ZrMe^+B(C_6F_4TBS)_4^-$ undergoes slow decomposition under an inert atmosphere to afford $[(1,2\text{-}Me_2Cp)_2ZrF]_2(\mu\text{-}F)^+B(C_6F_4TBS)_4^-$, which has been characterized by X-ray diffraction. The olefin polymerization activity and thermal stability of the zirconocene catalysts reaches a maximum when $B(C_6F_4TBS)_4^-$ and $B(C_6F_4TIPS)_4^-$ are used as counteranions. The polymerization activity of the zirconium constrained geometry complex also reaches a maximum in aromatic solvents when $B(C_6F_5)_4^-$ is used as the counteranion, apparently due to solvent coordination.

Introduction

Cationic group 4 metallocene complexes have been the subject of intensive research activity over the past decade because of their extraordinary characteristics as olefin polymerization catalysts.[1,2] Recent observations suggest that many of the properties of this class of highly active and selective homogeneous catalysts and the polymeric products derived therefrom are closely connected with the nature of the cation−anion tight ion-pairing (**A**).[3,4] Despite numerous elegant efforts to "engineer" the cationic portion of such catalysts,−[5] far less attention has been devoted to optimizing the charge-compensating anion (X^-) and to understanding the role of the ion-pairing in catalytic performance. As part of our continuing efforts to study the anion-related structure−reactivity aspects of this class of compounds, we were particularly interested in (fluoroaryl)borate

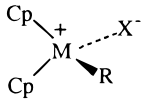

A

R = methyl or hydride; Cp = cyclopentadienyl-type ligand

[⊗] Abstract published in *Advance ACS Abstracts,* January 15, 1997.

(1) For recent reviews, see: (a) Bochmann, M. *J. Chem. Soc., Dalton Trans.* **1996**, 225−270. (b) Brintzinger, H. H.; Fischer, D.; Mülhaupt, R.; Rieger, B.; Waymouth, R. M. *Angew. Chem., Int. Ed. Engl.* **1995**, *34*, 1143−1170. (c) Kaminsky, W. *Catal. Today* **1994**, *20*, 257−271. (d) Möhring, R. C.; Coville, N. J. *J. Organomet. Chem.* **1994**, *479*, 1−29. (e) Marks, T. J. *Acc. Chem. Res.* **1992**, *25*, 57−65. (f) Jordan, R. F. *Adv. Organomet. Chem.* **1991**, *32*, 325−387.

(2) For some leading references in d^0 metal complex-catalyzed olefin polymerization, see: (a) Coates, G. W.; Waymouth, R. M. *Science* **1995**, *267*, 217−219. (b) Leclerc, M. K.; Brintzinger, H. H. *J. Am. Chem. Soc.* **1995**, *117*, 1651−1652. (c) Pellecchia, C.; Pappalardo, D.; Oliva, L.; Zambelli, A. *J. Am. Chem. Soc.* **1995**, *117*, 6593−6594. (d) Giardello, M. A.; Eisen, M. S.; Stern, C. L.; Marks, T. J. *J. Am. Chem. Soc.* **1995**, *117*, 12114−12129. (e) Kaminsky, W.; Engehausen, R.; Köpf, J. *Angew. Chem., Int. Ed. Engl.* **1995**, *34*, 2273−2275. (f) Spaleck, W.; Küber, F.; Winter, A.; Rohrmann, J.; Bochmann, B.; Antberg, M.; Dolle, V.; Paulus, E. F. *Organometallics* **1994**, *13*, 954−963. (g) Razavi, A.; Atwood. J. L. *J. Am. Chem. Soc.* **1993**, *115*, 7529−7530. (h) Chien, J. C. W.; Rausch, M. D.; Lin, G. Y.; Winter, H. H. *J. Am. Chem. Soc.* **1991**, *113*, 8569−8570. (i) Chien, J. C. W.; Tsai, W. M.; Rausch, M. D. *J. Am. Chem. Soc.* **1991**, *113*, 8570−8571. (j) Resconi, L.; Bossi, S.; Abis, L. *Macromolecules* **1990**, *23*, 4489−4491 (k) Ewen, J. A.; Jones, R. L.; Razavi, A.; Ferrara, J. D. *J. Am. Chem. Soc.* **1988**, *110*, 6255−6256. (l) Ewen, J. A. *J. Am. Chem. Soc.* **1984**, *106*, 6355−6364.

S0276-7333(96)00880-1 CCC: $14.00

anions and the ion-pairing behavior of complexes derived from them. We previously reported the successful strategy of using strong organo-Lewis acids such as $B(C_6F_5)_3$ to generate ion-paired cationic zirconocene complexes (eq 1), and we have studied their spectroscopic and structural properties, solution structural dynamic behavior, and catalytic performance in detail.[4a,b]

$$L_2ZrMe_2 + B(C_6F_5)_3 \xrightarrow{\text{toluene}} L_2ZrMe^+MeB(C_6F_5)_3^- \quad (1)$$

However, studies of related borate-based ($B(C_6F_5)_4^-$) zirconocene complexes were encumbered by the difficulty of isolating such complexes. Our attempted syntheses employing the reactions shown in eqs 2 and 3 invariably resulted in insoluble, oily materials containing a number of unidentified species. Nevertheless,

$$L_2ZrMe_2 + Ph_3C^+B(C_6F_5)_4^- \xrightarrow{\text{toluene}} L_2ZrMe^+B(C_6F_5)_4^- \quad (2)$$

$$L_2ZrMe_2 + {}^nBu_3NH^+B(C_6F_5)_4^- \xrightarrow{\text{toluene}} L_2ZrMe^+B(C_6F_5)_4^- + CH_4 + {}^nBu_3N \quad (3)$$

these mixtures, when freshly prepared, exhibit some of the highest reported olefin polymerization activities to date.[2d,i,j,4j,l] Clearly, such transformations warrant additional scrutiny, and additional examples of robust, weakly coordinating anions capable of stabilizing such highly electrophilic cations would be desirable to better understand ion-pairing behavior and the consequences on reactivity.

In the present contribution, we present a full account of our efforts to better define the nature of metallocenium−(fluoroaryl)borate ion-pairing and the polymerization catalytic consequences. We first report that changing the metallocene metal center from zirconium to thorium leads to isolation of the crystallographically characterizable, ion-paired complex $(Me_5Cp)_2ThMe^+B(C_6F_5)_4^-$ and that changing from the sandwich ligand framework (**A**) to a sterically more open half-sandwich ("constrained geometry") ligand framework (**B**) also leads to the isolation of ion-paired complexes.

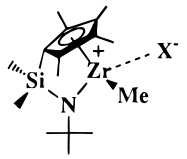

B

In a complementary effort to modify $B(C_6F_5)_4^-$ with lipophilic, sterically shielding, π-electron withdrawing protective groups, $B(C_6F_4TBS)_4^-$ and $B(C_6F_4TIPS)_4^-$ (TBS = *tert*-butyldimethylsilyl and TIPS = triisopropylsilyl) have been synthesized. These counteranions are expected to exhibit enhanced solubility in nonpolar solvents and modified metallocene coordination tendencies compared to $B(C_6F_5)_4^-$. We report a broad class of highly reactive cationic Zr and Th metallocene catalysts prepared using these anions.[6] Several $B(C_6F_5)_4^-$-based cationic zirconocene hydride complexes are also reported, and the complexity of eqs 2 and 3 is argued to arise from, among other factors, intramolecular C−H activation of the ligand framework. We next evaluate the relative coordinative tendencies of $MeB(C_6F_5)_3^-$, $B(C_6F_5)_4^-$, $B(C_6F_4TBS)_4^-$, and $B(C_6F_4TIPS)_4^-$ with respect to metallocene cations. In addition, the coordination of the neutral L_2MMe_2 metallocene precursors with the cationic metallocenes is studied and shown to compete significantly with borate counteranion coordination. Arene solvent coordination to the constrained geometry cation (**B**) is observed only when $B(C_6F_5)_4^-$ is the counterion. In addition, the relative thermal stabilities and olefin polymerization catalytic properties of the $B(C_6F_5)_4^-$-, $B(C_6F_4TBS)_4^-$-, and $B(C_6F_4TIPS)_4^-$-stabilized cationic complexes are investigated, and it is seen that they are generally more thermally stable and active for ethylene and propylene polymerization than the corresponding $MeB(C_6F_5)_3^-$-derived catalysts.

Experimental Section

Materials and Methods. All operations were performed with rigorous exclusion of oxygen and moisture in flamed Schlenk-type glassware on a dual-manifold Schlenk line or interfaced to a high-vacuum line (10^{-5} Torr) or in a dinitrogen-filled, Vacuum Atmospheres glovebox with a high-capacity atmosphere circulator (1−2 ppm O_2). Argon (Matheson, prepurified), ethylene (Matheson, CP), propylene (Matheson, PP), and dihydrogen (Linde) were purified by passage through a supported MnO oxygen-removal column and a Davison 4 A molecular sieve column. Hydrocarbon solvents (toluene, pentane) were distilled under nitrogen from Na/K alloy. Ether solvents (THF, Et_2O) were distilled under nitrogen from sodium benzophenone ketyl. All solvents were stored in vacuo over Na/K in Teflon-valved bulbs. 1-Hexene (Aldrich, 99%) was dried over Na/K for 1 h at room temperature, freeze−pump−thaw−degassed, and vacuum-transferred into a Teflon-

(3) (a) Chien, J. C. W.; Song, W.; Rausch, M. D. *J. Polym. Sci., Part A: Polym. Chem.* **1994**, *32*, 2387−2393. (b) Vizzini, J. C.; Chien, J. C. W.; Babu, G. N.; Newmark, R. A. *J. Polym. Sci., Part A: Polym. Chem.* **1994**, *32*, 2049−2056. (c) Giardello, M. A.; Eisen, M. S.; Stern, C. L.; Marks, T. J. *J. Am. Chem. Soc.* **1993**, *115*, 3326−3327. (d) Herfert, N.; Fink, G. *Makromol. Chem.* **1992**, *193*, 773−778.

(4) For leading references in chemisty of d^0 cationic group 4 and thorium metallocenes, see: (a) Yang, X.; Stern, C. L.; Marks, T. J. *J. Am. Chem. Soc.* **1994**, *116*, 10015−10031. (b) Deck, P. A.; Marks, T. J. *J. Am. Chem. Soc.* **1995**, *117*, 6128−6129. (c) Wu, Z.; Jordan, R. F.; Petersen, J. L. *J. Am. Chem. Soc.* **1995**, *117*, 5867−5868. (d) Bochmann, M.; Lancaster, S. J.; Robinson, O. B. *J. Chem. Soc., Chem. Commun.* **1995**, *20*, 2081−2082. (e) Erker, G.; Ahlers, W.; Frohlich, R. *J. Am. Chem. Soc.* **1995**, *117*, 5853−5854. (f) Siedle, A. R.; Newmark, R. A. *J. Organomet. Chem.* **1995**, *119*, 119−125. (g) Jia, L.; Yang, X.; Stern, C. L.; Marks, T. J. *Organometallics* **1994**, *13*, 3755−3757. (h) Sishta, C.; Hathorn, R. M.; Marks, T. J. *J. Am. Chem. Soc.* **1992**, *114*, 1112−1114. (i) Yang, X.; King, W. A.; Sabat, M.; Marks, T. J. *Organometallics* **1993**, *12*, 4254−4258. (j) Hlatky, G. G.; Eckman, R. R.; Turner, H. W. *Organometallics* **1992**, *11*, 1413−1416. (k) Ewen, J. A.; Elder, M. Eur. Pat. Appl. EP 427697, 1991. (l) Siedle, A. R.; Newmark, R. A.; Lamanna, W. M.; Schroepfer, J. N. *Polyhedron* **1990**, *9*, 301−308. (m) Turner, H. W.; Hlatky, G. G. PCT Int. Appl. WO 88/05793 (Eur. Pat. Appl. EP 211004, 1988).

(5) For leading references in zirconium catalysts with non-cyclopentadienyl ligands, see: (a) Flores, J. C.; Chien, J. C. W.; Rausch, M. D. *Organometallics* **1995**, *14*, 1827−1833. (b) Bowen, D. E.; Jordan, R. F.; Rogers, R. D. *Organometallics* **1995**, *14*, 3630−3635. (c) Black, D. G.; Swenson, D. C.; Jordan, R. F.; Rogers, R. D. *Organometallics* **1995**, *14*, 3539−3550. (d) Tjaden, E. B.; Swenson, D. C.; Jordan, R. F.; Petersen, J. L. *Organometallics* **1995**, *14*, 371−386. (e) van der Linden, A.; Schaverien, C. J.; Meijboom, N.; Ganter, C.; Orpen, A. G. *J. Am. Chem. Soc.* **1995**, *117*, 3008−3021. (f) Shapiro, P. J.; Cotter, W. D.; Schaefer, W. P.; Labinger, J. A.; Bercaw, J. E. *J. Am. Chem. Soc.* **1994**, *116*, 4623−4640. (g) Quan, R. W.; Bazan, G. C.; Kiely, A. F.; Schaefer, W. P.; Bercaw, J. E. *J. Am. Chem. Soc.* **1994**, *116*, 4489−4490. (h) Devore, D. D. Eur. Pat. Appl. 514828, 1991. (i) Stevens, J. C.; Timmers, F. J.; Wilson, D. R.; Schmidt, G. F.; Nickias, P. N.; Rosen, R. K.; Knight, G. W.; Lay, S. Y. Eur. Pat. Appl. 416815, 1990.

(6) For preliminary communications of part of these results, see: (a) Jia, L.; Yang, X.; Ishihara, A.; Marks, T. J. *Organometallics* **1995**, *14*, 3135−3137. (b) Yang, X.; Stern, C. L.; Marks, T. J. *Organometallics* **1991**, *10*, 840−842.

valved storage flask. Deuterated solvents were purchased from Cambridge Isotope Laboratories (all ≥99 atom % D), degassed and dried over Na/K alloy, and stored in resealable flasks. 1-Bromo-2,3,5,6-tetrafluorobenzene and bromopentafluorobenzene (Aldrich) were dried over molecular sieves. *tert*-Butyldimethylsilyl (TBS) triflate (98%), triisopropylsilyl (TIPS) triflate (98%), BCl_3 (1.0 M in hexane), and ^{n}BuLi (1.6 M in hexane) (Aldrich) were used as received. Triphenylcarbenium tetrakis(pentafluorophenyl)borate was received as a gift from Austin Chemicals Corp. and used as received.

The complexes $(Me_5Cp)_2ThMe_2$,[7] Cp_2ZrMe_2,[8] $(1,2\text{-}Me_2Cp)_2ZrMe_2$,[9] $(Me_5Cp)_2ZrMe_2$,[10] $[(Me_4Cp)SiMe_2(N^tBu)]ZrMe_2$,[11] and $[(Me_4Cp)SiMe_2(N^tBu)]ZrMe^+$ $MeB(C_6F_5)_3^-$ [11] were synthesized following established procedures.

Physical and Analytical Measurements. NMR spectra were recorded on either Varian Unity Plus 400 (FT, 400 MHz, ^{1}H; 100 MHz, ^{13}C), Gemini 300 (FT, 300 MHz, ^{1}H; 75 MHz, ^{13}C; 150 MHz, ^{19}F), or VXR-300 (FT 300 MHz, ^{1}H; 75 MHz, ^{13}C) spectrometers. Chemical shifts for ^{1}H and ^{13}C spectra were referenced using internal solvent resonances and are reported relative to tetramethylsilane. ^{19}F NMR were referenced to external $CFCl_3$. NMR experiments on air-sensitive samples were conducted in Teflon valve-sealed sample tubes (J. Young). Elemental analyses were performed by Oneida Research Service, Inc., Whitesboro, NY. GPC analyses of the polymer samples were performed at Akzo-Nobel Corporation Laboratories, Dobbs Ferry, NY.

Synthesis of $HC_6F_4Si^tBuMe_2$ (1a). In a 500 mL Schlenk flask, C_6HBrF_4 (14.8 g, 64.6 mmol) was dissolved in diethyl ether (300 mL) and cooled to −78 °C. ^{n}BuLi (40 mL, 1.6 M in hexanes) was then added dropwise over 0.5 h while the solution was stirred. Precipitation was immediately observed upon ^{n}BuLi addition. The reaction mixture was stirred for an additional 2 h before TBS triflate (17.0 g, 64.6 mmol) was injected into the suspension by a syringe. The flask was then slowly warmed to room temperature over the period of 8 h, and the resulting suspension was suction filtered through a frit. After the solvent was removed at 25 °C under reduced pressure, the nonvolatile liquid residue was distilled and a colorless liquid product was collected (bp 45 °C/0.8 mmHg). Yield: 14.0 g (82%). ^{1}H NMR (CCl_2D_2, 20 °C): δ 0.40 ("t", 6H), 0.93 (s, 9H), 7.10 (m, 1H). ^{19}F NMR (CCl_2D_2, 20 °C): δ −128.2 (m), −132.4 (m). ^{13}C NMR (CCl_2D_2, 20 °C): δ −3.7, 18.1, 26.5, 108.0 (t, J_{C-F} = 42 Hz), 116.5 (t, J_{C-F} = 48 Hz), 146.8 (d, J_{C-F} = 264 Hz), 150.4 (d, J_{C-F} = 262 Hz).

Synthesis of $HC_6F_4Si^iPr_3$ (1b). This synthesis followed a procedure similar to that for **1a** above, using C_6HBrF_4 (15.1 g, 65.9 mmol), ^{n}BuLi (41 mL, 1.6 M in hexanes), and TIPS triflate (21.0 g, 66.0 mmol). The product was distilled and collected at 62 °C/2 mmHg. Yield: 17.6 g (87%). ^{1}H NMR (CCl_2D_2, 20 °C): δ 0.98 (d, J = 7.5 Hz, 72H), 1.50 ("p", J = 7.5 Hz, 12H), 7.10 (m, 1H). ^{19}F NMR ($CDCl_3$, 20 °C): δ −128.2 (m), −132.4 (m).

Synthesis of $Li(Et_2O)_n^+B(C_6F_4Si^tBuMe_2)_4^-$ (2a). In a 500 mL Schlenk flask, **1a** (5.4 g, 20.4 mmol) was dissolved in diethyl ether (300 mL) and cooled to −78 °C. ^{n}BuLi (13.0 mL, 1.6 M in hexanes) was then added dropwise over 0.5 h while the solution was stirred. After an additional 2 h, BCl_3 (4.2 mL, 1.0 M in hexanes) was injected by a syringe and the reaction mixture was warmed to room temperature over the period of 16 h. The resulting suspension was then suction filtered through a Celite-covered frit. The volume of the mother liquid was next reduced to 75 mL, and pentane (250 mL) was layered on top of the solution. After 2 days, the recrystallized product was collected as large colorless crystals by filtration. Yield: 3.9 g (74%). ^{1}H NMR (C_6D_6, 20 °C): δ 0.20 (s, 24H), 0.80 (m, 12H), 0.82 (s, 36H), 3.05 (q, J = 7.1 Hz, 8H). ^{19}F NMR (C_6D_6, 20 °C): δ −129.4 (m), −133.8 (m).

Synthesis of $Li(Et_2O)_n^+B(C_6F_4Si^iPr_3)_4^-$ (2b). The reaction was carried out following a procedure similar to that for **2a** above, using **1b** (6.8 g, 22.2 mmol), ^{n}BuLi (10.5 mL, 2.5 M in hexanes), and BCl_3 (5.6 mL, 1.0 M in hexanes). Excess diethyl ether (∼800 mL) was needed to completely dissolve all of the product. The volume of the solution was reduced to 50 mL, and the white powder product was isolated after filtration and drying under vacuum (without further purification) in 72% yield (5.9 g). ^{1}H NMR ($CDCl_3$, 20 °C): δ 0.80 (t, J = 7.1 Hz, 12H), 1.08 (d, J = 7.5 Hz, 72H), 1.52 ("p", J = 7.5 Hz, 12H), 3.05(q, J = 7.1 Hz, 8H). ^{19}F NMR ($CDCl_3$, 20 °C): δ −131.3 (m), −132.1 (m).

Synthesis of $(C_6H_5)_3C^+B(C_6F_4Si^tBuMe_2)_4^-$ (3a). Compound **2a** (3.8 g, ∼3.1 mmol) and $(C_6H_5)_3CCl$ (1.14 g, 4.0 mmol) were loaded into a 500 mL Schlenk flask and suspended in pentane (250 mL). The orange suspension was stirred for 6 h at room temperature and then suction filtered through a frit. The orange solid which was collected was then dissolved in CH_2Cl_2, and the resulting suspension was filtered through a Celite-covered frit to remove LiCl. The volume of the filtrate was reduced to 50 mL, and pentane was added until the first precipitation was observed. The solution was then slowly cooled to −78 °C and stored for 12 h, and the solid product was collected by rapid filtration. The orange crystalline product was isolated in 86% yield (3.5 g). ^{1}H NMR (CCl_2D_2, 20 °C): δ 0.31 (s, 24H), 0.88 (s, 36H), 7.64 (d, J = 6.9 Hz, 6H), 7.85 (t, J = 6.9 Hz, 6H), 8.25 ("t", J = 6.9 Hz, 3H). ^{19}F NMR (CCl_2D_2, 20 °C): δ −129.0 (m), −132.5 (m). ^{13}C NMR (CCl_2D_2, 20 °C): δ −3.8, 17.8, 26.4, 108.4 (t, J_{C-F} = 42 Hz), 131.0, 140.2, 143.0, 144.0, 148.4 (d, J_{C-F} = 262 Hz), 148.6 (d, J_{C-F} = 262 Hz), 211.3. Anal. Calcd for $C_{67}H_{75}BF_{16}Si_4$: C, 61.55; H, 5.78. Found: C, 61.83; H, 5.61.

Synthesis of $(C_6H_5)_3C^+B(C_6F_4Si^iPr_3)_4^-$ (3b). This synthesis was carried out following a procedure similar to that for **3a** above, using compound **2b** (8.04 g, ∼5.6 mmol) and $(C_6H_5)_3CCl$ (1.7 g, 5.9 mmol). The orange crystalline product was isolated in 82% yield (6.8 g). ^{1}H NMR ($CDCl_3$): δ 1.09 (d, J = 7.5 Hz, 72H), 1.51 ("p", J = 7.5 Hz, 12H), 7.60 (d, J = 6.9 Hz, 6H), 7.85 (t, J = 6.9 Hz, 6H), 8.25 ("t", J = 6.9 Hz, 3H). ^{19}F NMR ($CDCl_3$, 20 °C): δ −131.3 (m), −132.1 (m). ^{13}C NMR ($CDCl_3$, 20 °C): δ 12.8, 18.8, 108.6 (t, J_{C-F} = 42 Hz), 130.6, 139.2, 142.4, 144.0, 147.8 (d, J_{C-F} = 26 Hz), 147.9 (d, J_{C-F} = 260 Hz), 211.3. Anal. Calcd for $C_{79}H_{99}BF_{16}Si_4$: C, 64.30; H, 6.76. Found: C, 64.57; H, 6.89.

Synthesis of $Cp_2ZrMe^+B(C_6F_4Si^tBuMe_2)_4^-$ (4a). Compound **3a** (390 mg, 0.30 mmol) and Cp_2ZrMe_2 (82 mg, 0.32 mmol) were loaded into a 50 mL reaction flask in the glovebox. The flask was attached to the vacuum line and evacuated, and toluene (20 mL) was condensed in the flask under vacuum. The flask was then backfilled with argon and warmed to room temperature, and the reaction mixture was stirred for 4 h. A white slurry formed during this period. After the slurry was collected by filtration and dried under vacuum, the pale yellow product was isolated. Yield: 292 mg (75%). ^{1}H NMR (C_6D_6, 60 °C): δ 0.23 (s, 24H), 0.56 (s, 3H), 0.85 (s, 36H), 5.75 (s, 10H). ^{19}F NMR (C_6D_6, 60 °C): δ −128.2 (b), −130.6 (b). ^{13}C NMR ($C_6D_4Cl_2$, 20 °C): δ −4.4, 17.2, 25.8, 49.6, 111.6 (t, J_{C-F} = 42 Hz), 114.8, 119.8, 147.0 (d, J_{C-F} = 262 Hz), 149.8 (d, J_{C-F} = 261 Hz). Anal. Calcd for $C_{59}H_{73}BF_{16}Si_4Zr$: C, 54.49; H, 5.66. Found: C, 54.30; H, 5.35.

Synthesis of $Cp_2ZrMe^+B(C_6F_4Si^iPr_3)_4^-$ (4b). This synthesis was carried out following a procedure similar to that for **4a** above, using compound **3b** (405 mg, 0.27 mmol) and Cp_2ZrMe_2 (68 mg, 0.27 mmol). The pale yellow product was isolated in 83% yield (332 mg). ^{1}H NMR (C_6D_6, 60 °C): δ 0.54 (s, 3H), 1.01 (d, J = 7.5 Hz, 72H), 1.43 ("p", J = 7.5 Hz, 12H), 5.75 (s, 10H). ^{19}F NMR (C_6D_6, 60 °C): δ −130.1 (b), −131.4

(7) Fagan, P. J.; Manriquez, J. M.; Maatta, E. A.; Seyam, A. M.; Marks, T. J. *J. Am. Chem. Soc.* **1981**, *103*, 6650−6667.
(8) Samuel, E.; Rausch, M. D. *J. Am. Chem. Soc.* **1973**, *95*, 6263−6267.
(9) Smith, G. M. Ph.D. Thesis, Northwestern University, Evanston, IL, 1985.
(10) Manriquez, J. M.; McAlister, D. R.; Sanner, R. D.; Bercaw, J. E. *J. Am. Chem. Soc.* **1978**, *100*, 2716−2724.
(11) Lanza, G.; Fragala, I. L.; Fu, P.-F.; Marks, T. J.; Wilson, D. R.; Rudolph, P. R. Manuscript in preparation.

(b). ^{13}C NMR ($C_6D_4Cl_2$, 20 °C): δ 12.0, 19.2, 111.6 (t, J_{C-F} = 42 Hz), 114.8, 120, 146.6 (d, J_{C-F} = 259 Hz), 150 (d, J_{C-F} = 262 Hz). Anal. Calcd for $C_{71}H_{97}BF_{16}Si_4Zr$: C, 58.06; H, 6.66. Found: C, 58.32; H, 6.79.

Synthesis of (1,2-Me$_2$Cp)$_2$ZrMe$^+$B(C$_6$F$_4$Si^{t}BuMe$_2$)$_4^-$ (5a). Compound **3a** (390 mg, 0.30 mmol) and (1,2-Me$_2$Cp)$_2$ZrMe$_2$ (92 mg, 0.30 mmol) were loaded into a 50 mL reaction flask in the glovebox. The flask was attached to the vacuum line and evacuated, and toluene (20 mL) was condensed into the flask under vacuum. The flask was then backfilled with argon and warmed to room temperature. The reaction mixture was stirred for 6 h, during which time a pale yellow solution formed. The volume of the solution was reduced to ~5 mL, and 20 mL of pentane was condensed into the flask to precipitate the product. After this was collected by filtration and dried under vacuum, the off-white product was isolated in 78% yield (317 mg). ^{1}H NMR (C_6D_6, 20 °C): δ 0.21(s, 24H), 0.34 (s, 3H), 0.83 (s, 36H), 1.37 (s, 6H), 1.61 (s, 6H), 5.00 (b, 2H), 5.69 (b, 2H), 5.97 (t, 2H). ^{13}C NMR (C_6D_6, 20 °C): δ −3.9, 12.5, 17.7, 26.4, 45.9, 108.1 (t, J_{C-F} = 42 Hz), 110.1, 111.8, 119.8, 133.5, 147.7 (d, J_{C-F} = 262 Hz), 148.0 (d, J_{C-F} = 262 Hz). Anal. Calcd for $C_{63}H_{81}BF_{16}Si_4Zr$: C, 55.78; H, 6.02. Found: C, 55.56; H, 6.01.

Synthesis of (1,2-Me$_2$Cp)$_2$ZrMe$^+$B(C$_6$F$_4$Si^{i}Pr$_3$)$_4^-$ (5b). This synthesis was carried out following a procedure similar to that for **5a** above, using compound **3b** (420 mg, 0.28 mmol) and (1,2-Me$_2$Cp)$_2$ZrMe$_2$ (87 mg, 0.28 mmol). The off-white product was isolated in 78% yield (332 mg). ^{1}H NMR (toluene-d_8, 20 °C): δ 0.37 (s, 3H), 1.08 (d, J = 7.5 Hz, 72H), 1.43 (s, 6H), 1.51 ("t", J = 7.5 Hz, 12H), 1.73 (s, 6H), 5.08 (b, 4H), 5.75 (b, 4H), 6.01 (t, J = 1.0 Hz, 2H). ^{13}C NMR (toluene-d_8, 20 °C): δ 12.0, 12.8, 19.2, 47.0, 109.1 (t, J_{C-F} = 42 Hz), 110.1, 113.8, 121.4, 149.8 (d, J_{C-F} = 262 Hz), 150.7 (d, J_{C-F} = 262 Hz). Anal. Calcd for $C_{75}H_{105}BF_{18}Si_4Zr$: C, 59.07; H, 6.94. Found: C, 59.34; H, 6.94.

Synthesis of (1,2-Me$_2$Cp)$_2$ZrH$^+$B(C$_6$F$_5$)$_4^-$ (5c). This synthesis was carried out following a procedure similar to that for **5a** above, except that the reaction was carried out under 1.0 atm of H_2 using compound $Ph_3C^+B(C_6F_5)_4^-$ (258 mg, 0.28 mmol) and (1,2-Me$_2$Cp)$_2$ZrMe$_2$ (87 mg, 0.28 mmol). The off-white product was isolated in 78% yield (212 mg). ^{1}H NMR (C_6D_6/THF-d_8, 20 °C): δ 1.71 (s, 12H), 5.71 (d, J = 2.8 Hz, 4H), 5.78 (t, J = 2.8 Hz, 2H), 9.4 (s, 1H). ^{19}F NMR (C_6D_6, 60 °C): δ −132.3 (b), −163.5 (t, J = 20 Hz), −167.2 (b). Anal. Calcd for $C_{38}H_{19}BF_{20}Zr$: C, 47.66; H, 2.00. Found: C, 47.11; H, 1.60.

Synthesis of (Me$_5$Cp)$_2$ZrH$^+$B(C$_6$F$_4$Si^{t}BuMe$_2$)$_4^-$ (6a). This synthesis was carried out following a procedure similar to that for **5a** above, except that the reaction was carried out under 1.0 atm of H_2 using **3a** (400 mg, 0.31 mmol) and (Me$_5$Cp)$_2$ZrMe$_2$ (120 mg, 0.31 mmol). Yield: 318 mg (72%). ^{1}H NMR (C_6D_6, 20 °C): δ 0.25 (s, 24H), 0.87 (s, 36H), 1.63 (s, 30H), 7.90 (b, 1H). ^{13}C NMR (C_6D_6, 20 °C): δ −3.9, 11.2, 17.7, 26.5, 110.1 (t, J_{C-F} = 42 Hz), 122.5, 148.1 (d, J_{C-F} = 262 Hz), 148.2 (d, J_{C-F} = 262 Hz). Anal. Calcd for $C_{68}H_{91}BF_{16}Si_4Zr$: C, 57.24; H, 6.43. Found: C, 56.87; H, 6.46.

Synthesis of (Me$_5$Cp)$_2$ZrH$^+$B(C$_6$F$_4$Si^{i}Pr$_3$)$_4^-$ (6b). This synthesis was carried out following a similar procedure to that for **6a** above, using compound **3b** (368 mg, 0.25 mmol) and (Me$_5$Cp)$_2$ZrMe$_2$ (98 mg, 0.25 mmol). Yield: 311 mg (78%). ^{1}H NMR (C_6D_6, 20 °C): δ 1.12 (d, J = 7.5 Hz, 72H), 1.50 ("p", J = 7.5 Hz, 12H), 1.72 (s, 30H), 7.96 (b, 1H). ^{13}C NMR (toluene-d_8, 20 °C): δ 12.0, 12.5, 18.8, 109.8 (t, J_{C-F} = 42 Hz), 111.9, 148.2 (d, J_{C-F} = 262 Hz), 148.0 (d, J_{C-F} = 262 Hz). Anal. Calcd for $C_{80}H_{115}BF_{16}Si_4Zr$: C, 60.46; H, 7.33. Found: C, 60.56; H, 6.98.

Synthesis of (Me$_5$Cp)$_2$ZrH$^+$B(C$_6$F$_5$)$_4^-$ (6c). This synthesis was carried out following a procedure similar to that for **6a** above. The reagents $Ph_3C^+B(C_6F_5)_4^-$ (286 mg, 0.31 mmol) and (Me$_5$Cp)$_2$ZrMe$_2$ (120 mg, 0.31 mmol) were used. Yield: 220 mg (68%). ^{1}H NMR (C_6D_6, 20 °C): δ 1.38 (s, 30H), 7.41 (b, 1H). ^{19}F NMR (C_6D_6, 20 °C): −133.9 (b), −161.0 (t, J = 20 Hz), 167 (b). Anal. Calcd for $C_{44}H_{31}BF_{20}Zr$: C, 50.73; H, 3.00. Found: C, 51.69; H, 2.99.

Synthesis of [(Me$_4$Cp)SiMe$_2$(N^{t}Bu)]ZrMe$^+$B(C$_6$F$_4$Si^{t}BuMe$_2$)$_4^-$ (7a). Compound **3a** (362 mg, 0.28 mmol) and [(Me$_4$Cp)SiMe$_2$(N^{t}Bu)]ZrMe$_2$ (103 mg, 0.28 mmol) were loaded into a 50 mL reaction flask in the glovebox. The flask was attached to the vacuum line and evacuated, and toluene (30 mL) was condensed into the flask under vacuum. The flask was then backfilled with argon, warmed to room temperature, and stirred for 4 h. The orange slurry gradually turned to a transparent colorless solution during this time period. The volume of toluene was next reduced to 10 mL, and 20 mL of hexanes was condensed into the flask at −78 °C. A clear solution formed at room temperature, and the solution was slowly cooled to −78 °C and kept at this temperature for 12 h. The pale yellow crystalline product was isolated by quick filtration through a course frit and was dried under vacuum overnight. Yield: 123 mg (32%). ^{1}H NMR (C_6D_6, 60 °C): δ 0.21 (s, 3H), 0.23 (s, 24H), 0.28 (s, 3H), 0.35 (s, 3H), 0.86 (s, 36H), 1.23 (s, 9H), 1.49 (s, 3H), 1.83 (s, 3H), 1.97 (s, 3H), 2.05 (s, 3H). ^{13}C NMR (C_6D_6, 20 °C): δ −4.4 (TBS), 5.7 (Si*Me*$_2$), 9.0 (Si*Me*$_2$), 11.3 (*Me*$_4$Cp), 12.4 (*Me*$_4$Cp), 13.2 (*Me*$_4$Cp), 14.9 (*Me*$_4$Cp), 17.2, 18.7 (*C*Me$_3$), 25.8 (TBS), 30.8 (C*Me*$_3$), 57.2 (Zr−*Me*), 102.9 (Cp), 108.0 (t, J_{C-F} = 42 Hz, C_6F_5), 131.9 (Cp), 132.1 (Cp), 132.4 (Cp), 133.6 (Cp), 148.9 (d, J_{C-F} = 262 Hz, C_6F_4), 150.0 (d, J_{C-F} = 262 Hz, C_6F_4). Anal. Calcd for $C_{64}H_{90}BNF_{16}Si_5Zr$: C, 54.16; H, 6.39; N, 0.99. Found: C, 54.46; H, 5.93; N, 0.62.

Synthesis of [(Me^{4}Cp)SiMe$_2$(N^{t}Bu)]ZrMe$^+$B(C$_6$F$_4$Si^{i}Pr$_3$)$_4^-$ (7b). Compound **3b** (412 mg, 0.28 mmol) and [(Me$_4$Cp)SiMe$_2$(N^{t}Bu)]ZrMe$_2$ (104 mg, 0.28 mmol) were loaded into a 50 mL reaction flask in the glovebox. The flask was connected to the vacuum line and evacuated, and benzene (30 mL) was condensed into the flask under vacuum. The flask was next backfilled with argon, warmed to room temperature, and stirred for 4 h. The orange slurry gradually became a transparent, colorless solution during this time period. Benzene was then removed *in vacuo*, and 20 mL of hexanes was condensed into the flask at −78 °C. The slurry was stirred at room temperature for 1 h and was filtered. The off-white product was isolated by filtration and dried under vacuum overnight. Yield: 332 mg (75%). ^{1}H NMR (C_6D_6, 60 °C): δ 0.16 (s, 3H), 0.23 (s, 3H), 0.32 (s, 3H), 1.05 (d, J = 7.6 Hz, 72H), 1.22 (s, 9H), 1.47 (b, 12H), 1.54 (s, 3H), 1.82 (s, 3H), 1.97 (s, 3H), 2.04 (s, 3H). ^{13}C NMR (C_6D_6, 20 °C): δ 4.0 (TIPS), 5.7 (Si*Me*$_2$), 9.0 (Si*Me*$_2$), 11.3 (*Me*$_4$Cp), 12.3 (*Me*$_4$Cp), 13.3 (*Me*$_4$Cp), 14.9 (*Me*$_4$Cp), 18.7 (TIPS), 30.8 (*C*Me$_3$), 40.2 (C*Me*$_3$), 57.2 (Zr−*Me*), 102.6 (Cp), 108.0 (t, J_{C-F} = 42 Hz, C_6F_5), 131.9 (Cp), 132.1 (Cp), 132.4 (Cp), 133.6 (Cp), 149.7 (d, J_{C-F} = 262 Hz), 150.0 (d, J_{C-F} = 262 Hz). Anal. Calcd $C_{76}H_{114}BNF_{16}Si_5Zr$: C, 57.48; H, 7.24; N, 0.88. Found: C, 57.86; H, 6.62; N, 0.46.

Synthesis of [(Me$_4$Cp)SiMe$_2$(N^{t}Bu)]ZrMe$^+$B(C$_6$F$_5$)$_4^-$·C$_6$H$_6$ (7c). This synthesis was carried out following a procedure similar to that for **7b** above, using $Ph_3C^+B(C_6F_5)_4^-$ (440 mg, 0.477 mmol) and [(Me$_4$Cp)SiMe$_2$(N^{t}Bu)]ZrMe$_2$ (176 mg, 0.477 mmol). Yield: 413 mg (84%). ^{1}H NMR (C_6D_6, 20 °C): δ −0.45 (s, 3H), 0.13 (s, 3H), 0.23 (s, 3H), 0.78 (s, 9H), 1.37 (s, 3H), 1.47 (s, 3H), 1.58 (s, 3H), 1.65 (s, 3H). ^{19}F NMR (C_6D_6, 20 °C): δ −132.2 (b), −162.2 (t, J = 19 Hz), −166.2 (d, J = 16 Hz). ^{13}C NMR (C_6D_6, HMQC, 20 °C): δ 5.1 (Si*Me*$_2$), 10.2 (Si*Me*$_2$), 10.4 (*Me*$_4$Cp), 11.1 (*Me*$_4$Cp), 12.5 (*Me*$_4$Cp), 15.4 (*Me*$_4$Cp), 32.2 (Zr−*Me*), 33.6 (C*Me*$_3$). Anal. Calcd for $C_{46}H_{36}BNF_{20}SiZr$ (**7c**·C_6H_6): C, 49.60; H, 3.35; N, 1.26. Found: C, 49.05; H, 3.45; N, 1.26.

Synthesis of (Me$_5$Cp)$_2$ThMe$^+$B(C$_6$F$_4$Si^{t}BuMe$_2$)$_4^-$ (8a). This synthesis was carried out following a procedure similar to that for **5a** above, using **3a** (368 mg, 0.28 mmol) and (Me$_5$Cp)$_2$ThMe$_2$ (150 mg, 0.28 mmol). Yield: 72% (318 mg). ^{1}H NMR (C_6D_6, 20 °C): δ 0.25 (s, 24H), 0.53 (s, 3H), 0.87 (s, 36H), 1.75 (s, 30H). ^{19}F NMR (C_6D_6, 20 °C): −128.2 (b), −130.4 (b). ^{13}C NMR (C_6D_6, 20 °C): δ −3.7, 10.8, 17.8, 26.5, 77.0, 109.1 (t, J_{C-F} = 42 Hz), 129.2, 148.0 (d, J_{C-F} = 262 Hz), 151.0 (d,

J_{C-F} = 258 Hz). Anal. Calcd for $C_{68}H_{93}BF_{16}Si_4Th$: C, 52.20; H, 6.28. Found: C, 52.35; H, 5.84.

Synthesis of $(Me_5Cp)_2ThMe^+B(C_6F_4Si^iPr_3)_4^-$ (8b). This synthesis was carried out following a procedure similar to that for **5a** above, using **3b** (412 mg, 0.28 mmol) and $(Me_5Cp)_2ThMe_2$ (150 mg, 0.28 mmol). Yield: 382 mg (78%). ^{1}H NMR (C_6D_6, 20 °C): δ 0.59 (s, 3H), 1.09 (d, J = 7.4 Hz, 72H), 1.51 ("p", J = 7.4 Hz, 12H), 1.75 (s, 30H), 7.96 (b, 1H). ^{19}F NMR (C_6D_6, 20 °C): −128.6 (b), −132.2 (b). ^{13}C NMR (C_6D_6, 20 °C): δ 10.7, 12.1, 18.4, 77.1, 109.8 (t, J_{C-F} = 42 Hz), 129.5, 148.2 (d, J_{C-F} = 262 Hz), 150.0 (d, J_{C-F} = 261 Hz). Anal. Calcd for $C_{81}H_{117}BF_{16}Si_4Th$: C, 55.59; H, 6.74. Found: C, 55.35; H, 6.52.

Synthesis of $(Me_5Cp)_2ThMe^+B(C_6F_5)_4^-$ (8c). This synthesis was carried out following a similar procedure to that for **5a** above, using $Ph_3C^+B(C_6F_5)_4^-$ (300 mg, 0.325 mmol) and $(Me_5Cp)_2ThMe_2$ (173 mg, 0.325 mmol) with benzene as the solvent. Yield: 303 mg (78%). ^{1}H NMR (C_6D_6, 20 °C): δ 0.34 (s, 3H), 1.54 (s, 12H). ^{19}F (C_6D_6, 20 °C): −132.6 (b, s, 8F), −162.11 (t, J_{F-F} = 21.1 Hz, 4F), −166.0 (m, 8F). ^{13}C (CP-MAS): δ 10.1 (*Me*$_5$Cp), 78.1 (Th−*Me*). Anal. Calcd for $C_{45}H_{33}BF_{20}Th$: C, 45.17; H, 2.78. Found: C, 44.53; H, 2.88.

Synthesis of $[(Me_5Cp)_2ThMe]_2(\mu\text{-}Me)^+B(C_6F_5)_4^-$ (9). Compound **8c** (103 mg, 0.086 mmol) and $(Me_5Cp)_2ThMe_2$ (69 mg, 130 mmol) were loaded into a 25 mL reaction flask in the glovebox. The flask was then transferred to the vacuum line and evacuated, and benzene (10 mL) was condensed into the flask. The reaction mixture was stirred for 4 h at room temperature. The resulting slurry was then filtered through a frit, and the colorless crystalline product was isolated after drying under vacuum. Yield: 105 mg (71%). ^{1}H NMR (toluene-d_8, −27 °C): δ −1.22 (s, 3H), 0.05 (s, 6H), 1.72 (s, 30H). ^{13}C NMR (CPMAS, 20 °C): δ 10.9 (*Me*$_5$C$_5$), 56.6 (bridging *Me*), 76.5 (terminal *Me*), 127.3 (*C*$_5$Me$_5$). Anal. Calcd for $C_{67}H_{69}BF_{20}Th_2$: C, 46.54; H, 4.02. Found: C, 46.31; H, 4.04.

Synthesis of $[(1,2\text{-}Me_2Cp)_2ZrMe]_2(\mu\text{-}Me)^+B(C_6F_4TBS)_4^-$ (10). Compound **5a** (200 mg, 0.147 mmol) and a stoichiometric excess of $(1,2\text{-}Me_2Cp)_2ZrMe_2$ (80 mg, 0.260 mmol) were loaded into a 25 mL reaction flask in the glovebox. The flask was then connected to the vacuum line and evacuated, and toluene (10 mL) was condensed into the flask. The reaction mixture was stirred for 4 h at room temperature. The resulting slurry was then filtered through a frit, and the colorless crystalline product was isolated after drying under vacuum. Yield: 103 mg (42%). ^{1}H NMR ($C_6D_4Cl_2$, 20 °C): δ −1.47 (s, 3H), −0.23 (s, 6H), 0.13 (s, 24H), 0.72 (s, 36H), 1.61 (s, 12H), 1.80 (s, 12H), 5.38 (t, J = 2.8 Hz), 5.58 ("t", 8H). ^{19}F (C_6D_6, 20 °C): −128.6 (b), −132.2 (b). ^{13}C NMR ($C_6D_4Cl_2$/C_6D_6, 20 °C): δ −6.0, 10.8, 11.1, 15.4, 20.5, 24.1, 39.9, 104.5, 106.2 (t, J_{C-F} = 48 Hz), 109.3, 112.5, 147.1 (d, J_{C-F} = 262 Hz), 147.2 (d, J_{C-F} = 262 Hz). Anal. Calcd for $C_{79}H_{105}BF_{16}Si_4Zr_2$: C, 55.59; H, 6.74. Found: C, 55.35; H, 6.52.

Equilibration between 5a, $(1,2\text{-}Me_2Cp)_2ZrMe_2$, and 10. The three title species are in equilibrium in benzene solution, and the equilibrium constant was measured at 19 °C by ^{1}H NMR, using the following procedure. Solutions of **5a** (10.0 mg, 0.0073 mmol in 1.00 mL of C_6D_6) and $(1,2\text{-}Me_2Cp)_2ZrMe_2$ (6.0 mg, 0.0195 mmol in 2.65 mL of C_6D_6) were prepared in the glovebox. In the next step, 0.1 mL + 0.1 mL, 0.1 mL + 0.2 mL, and 0.2 mL + 0.1 mL of the above two solutions were loaded into each of three NMR tubes. Additional C_6D_6 was then added to make the total liquid volume of each sample 0.8 mL. The concentration ratio of each species in the solution was determined using eq 4, where I_a and I_b are the integated

$$[\mathbf{5a}]:[(1,2\text{-}Me_2Cp)_2ZrMe_2]:[\mathbf{10}] = [n(I_a/2 + I_b) - I_b]:I_a/2:I_b \quad (4)$$

values of the signals at δ −0.36 and −1.27 ppm, corresponding to neutral terminal Zr−Me$_2$ and bridging Zr(μ-Me)Zr groups, respectively, and n is the initial mole ratio of **5a** and $(1,2\text{-}Me_2Cp)_2ZrMe_2$. The direct integral value of the signal corresponding to Zr^+−Me could not be used because it overlaps with the Si−Me signal. The sum of the concentrations of the three species equals the sum of the initial concentrations of **5a** and $(1,2\text{-}Me_2Cp)_2ZrMe_2$. The concentration of each species in the solution was then determined from the total concentration, and the concentration ratio was deduced from eq 4. Each of the three samples was then diluted to 1.6 mL, and the above measurement was repeated.

Study of Solution Dynamic Behavior of 5a, 5b, and 7c Using Variable Temperature NMR Spectroscopy. The solution structural dynamic processes involving the title compounds are all in the slow exchange limit at temperatures below 55 °C. The rate constant for the exchange process at each temperature was determined using modified Bloch eq 5,[12] where $\Delta W = W - W_o$ and W is the line width at half-

$$k = \pi(\Delta W) \quad (5)$$

height of the signals of interest at each individual temperature, and W_o is the natural line width at half-height, which was measured at 20 °C and confirmed by observing no change of the line width at 10 °C. The same measurements were undertaken on samples of various concentrations over a 4-fold range, and no concentration dependence of the processes was detected.

Solution Phase Thermal Stabilities of Complexes 4−8. A C_6D_6 solution of each complex was monitored by ^{1}H and ^{19}F NMR spectroscopy at 70 and 100 °C. Complexes **4** and **8** decomposed rapidly at 70 °C on a time scale of ∼0.5 h. Complexes **5**, **6**, **7a**, and **7b** do not undergo noticeable decomposition over the course of 1 h at 100 °C and only give evidence of decomposition at higher temperatures (130 °C) or on prolonged heating at 100 °C. Compound **7c** is less stable and has a half-life of ∼0.5 h at 80 °C. These decomposition processes are complicated, and it was not possible to characterize the products in detail. However, a toluene solution of **5a** stored at room temperature for several weeks resulted in precipitatation of crystallographically characterizable single crystals of $[(1,2\text{-}Me_2Cp)_2ZrF]_2(\mu\text{-}F)^+B(C_6F_4TBS)_4^-$ (**11**).

^{13}C Scrambling between 8a and $(Me_5Cp)_2Th(^{13}CH_3)_2$. A mixture of the title compounds was shaken together in C_6D_6. After 1 h at room temperature, ^{1}H NMR spectroscopy revealed that the ^{13}C labels were evenly distributed among the Th−Me positions.

Ethylene Polymerization Experiments. Ethylene polymerizations were carried out in flamed 250 mL round-bottom flasks, using 100 mL of toluene as the solvent under 1.0 atm ethylene pressure and following the procedures described previously.[4a] These processes are designed to assure rapid mixing of the monomer with the catalyst solution and to minimize mass transport effects on the measured rates.

Propylene Polymerization Experiments. Propylene polymerizations were carried out in flamed 100 mL round-bottom flasks, using 40 mL of toluene as the solvent under 1.0 atm propylene pressure and following the procedures described previously.[2d]

Formation of $(Me_5Cp)_2Th(\eta^3\text{-allyl})^+B(C_6F_5)_4^-$ (12). A toluene-d_8 solution of **8c** (∼2 mg) in a NMR tube was prepared in the glovebox, evacuated at −78 °C on the high-vacuum line, and exposed to 1.0 atm of propylene at 0 °C. After 15 min at 0 °C, the ^{1}H NMR spectrum showed that **8c** was quantitatively converted to an allylic complex, with elimination of NMR-detectable methane. ^{1}H NMR (toluene-d_8, 25 °C): δ 6.12 (m, 1H), 3.06 (d, J = 13.8 Hz, 2 H), 2.53 (d, J = 8.8 Hz, 2H), 1.45 (s, 30H).

X-ray Crystallographic Studies of Complexes 8c and 11. Crystals of **8c** suitable for diffraction studies were grown by slow diffusion of pentane into a saturated benzene solution

(12) (a) Sandstrom, J. *Dynamic NMR Spectroscopy*; Academic Press: New York, 1982; pp 77−92. (b) Kaplan, J. I.; Fraenkel, G. *NMR of Chemically Exchanging Systems*; Academic Press: New York, 1980; pp 71−128.

Table 1. Summary of the Crystal Structure Data for $(Me_5Cp)_2ThMe^+$ $B(C_6F_5)_4^-$ (8c) and $[(1,2\text{-}Me_2Cp)_2ZrF]_2(\mu\text{-}F)^+B(C_6F_4TBS)_3^-$ (11)

complex	8c	11
formula	$ThC_{45}H_{33}BF_{20}\cdot(C_6H_6)_{2.5}$	$Zr_2Si_4F_{19}C_{88}BH_{87}$
crystal system	monoclinic	triclinic
space group	$P2_1/c$	$P\bar{1}$
a, Å	18.390(7)	15.840(6)
b, Å	16.444(4)	15.979(7)
c, Å	18.731(6)	20.79(1)
α, deg	90	96.56(4)
β, deg	99.20(3)	101.22(3)
γ, deg	90	106.26(3)
V, Å^3	5592(3)	4875(4)
Z	4	2
d(calcd), g/cm^3	1.653	1.23
crystal size, mm	0.4 × 0.4 × 0.4	0.05 × 0.03 × 0.06
color, habit	colorless, transparent	yellow, transparent
diffractometer	Enraf-Nonius, CAD4	Enraf-Nonius, CAD4
temp, °C	−120	−120
μ, cm^{-1}	28.62	3.37
transmission factors range	0.411−0.256 (numerical)	0.878−0.978
radiation	graphite monochromator; Mo Kα:λ = 0.710 69 Å	
scan type	$\theta-2\theta$	$\omega-\theta$
2θ range, deg	2−42 ($+h,+k,\pm l$)	2.8−45.9
intensities (unique, R_i)	6609 (5989, 0.015)	13 976 (13 532, 0.072)
intensities >2.58$\sigma(I)$	4074	
intensities >3.00$\sigma(I)$		6197
no. of params	672	607
R	0.035	0.09
R_w for $w = 1/s^2(F_o) + rF_o^2$	0.037 (r = 0.010)	0.111
max density in DF map, e/Å^3	1.03	1.26

of **8c** at room temperature, and crystals of **11** suitable for diffraction studies were retrieved from a decomposed solution of **5a** in toluene. Both were mounted on thin glass fibers, after protecting with a layer of Paratone oil (Exxon, degassed at 100 °C for 10 h under high vacuum). Data were collected on an Enraf-Nonius CAD4 diffractometer at −120 °C. Final cell dimensions were obtained by a least-squares fit to the automatically centered settings for 25 reflections. Three reference reflections monitored during data collection for each crystal showed no significant variations. Intensity data were all corrected for absorption, anomalous dispersion, and Lorentz and polarization effects. The space group choice for each complex was unambiguously determined.[13] Crystallographic data are summarized in Table 1.

The structure of complex **8c** was solved by Patterson methods. The correct thorium atom position was automatically determined from a Patterson map (SHELX-86).[14] Subsequent least-squares difference Fourier calculations (SHELX-76) revealed atomic positions for the remaining non-hydrogen atoms. The hydrogen atoms were included as fixed contributors in "idealized" positions. The hydrogen atoms of the benzene solvent molecules were not included in the structure refinement. The non-hydrogen atoms were refined with anisotropic thermal coefficients, and common isotropic thermal parameters were varied for hydrogen atoms. The highest peaks in the final difference Fourier map were in the vicinity of the thorium position. A final analysis of the variance between observed and calculated structure factors showed a slight dependence on sin θ.

The structure of **11** was solved by direct methods and expanded using Fourier techniques. The carbon and boron atoms were refined isotropically. The remaining non-hydrogen atoms were refined anisotropically. The hydrogen atoms were not included in the structure factor calculations. The final cycle of full-matrix least-squares refinement was based on 6197 observed reflections ($I > 3.00\sigma(I)$) and 607 variable parameters. All calculations were performed using the TEXSAN crystallographic software package of Molecular Structure Corp.

(13) Cromer, D. T.; Waber, J. T. *International Tables for X-ray Crystallogrophy*; The Kynoch Press: Birmingham, England, 1974; Vol. IV, p 149.

(14) (a) Sheldrick, G. M. SHELXS-86. In *Crystallographic Computing*; Sheldrick, G. M., Kruger, C., Goddard, R., Eds.; Oxford University Press: Oxford, 1985; pp 175−189. (b) Sheldrich, G. M. *SHELXS-76 A Program for Crystal Structure Determination*; University Chemical Laboratory: Cambridge, England, 1976.

Results and Discussion

The goal of this study was to understand the role of the charge-compensating counteranion in stabilizing and activating cationic Zr and Th metallocene complexes, the solution ion-pairing properties associated with this interaction, and, ultimately, to probe for "ideal" situations in which the ion-paired complexes exhibit optimal olefin polymerization activity, solubility, and thermal stability. It will be seen that several broad new classes of ion-paired, cationic Zr and Th complexes with a variety of counteranions can be efficiently synthesized. Comparison of the spectroscopy, solution dynamic properties, coordinative behavior, and polymerization activity of these complexes facilitates a considerably deeper understanding of cation architecture−anion architecture−reactivity relationships.

I. Cationic Ion-Paired Alkyl- and Hydridozirconium and Alkylthorium (Fluoroaryl)borate Complexes. Synthesis and Spectroscopy. A. Synthesis of Functionalized Borate Anions $B(C_6F_4TBS)_4^-$ and $B(C_6F_4TIPS)_4$. The quest for noncoordinating anions has been a long standing challenge in inorganic chemical research.[15] Due to the extremely high electrophilicity of the Lewis base−free cationic zirconocene and thorocene complexes, an effective counteranion must necessarily be chemically robust and exceptionally resistant to electrophilic attack, in addition to other recognized requirements for weakly coordinating anions.[15] In fact, only a small number of anions stabilize

(15) (a) Jelinek, T.; Baldwin, P.; Scheidt, W. R.; Reed, C. A. *Inorg. Chem.* **1993**, *32*, 1982−1990. (b) Strauss, S. H. *Chem. Rev.* **1993**, *93*, 927−942. (c) Seppelt, K. *Angew. Chem., Int. Ed. Engl.* **1993**, *32*, 1025−1027. (d) Bochmann, M. *Angew. Chem., Int. Ed. Engl.* **1992**, *31*, 1181−1182.

Scheme 1

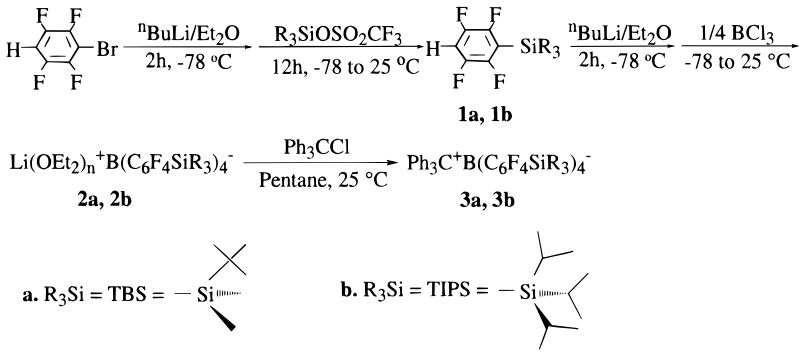

the present highly electrophilic cations. On the basis of our earlier success using the (fluoroaryl)borate $MeB(C_6F_5)_3^-$ as the counteranion for zirconocenium ions[4a,b] and observations that reactions of the trityl or ammonium salts of $B(C_6F_5)_4^-$ with neutral zirconocene dialkyls afford highly active olefin polymerization catalysts,[2d,i,j,4j,l] silyl-functionalized (fluoroaryl)borate anions **3a** and **3b** were designed. A high level of aryl group fluorination was retained to ensure delocaliztion/neutralization of the negative charge. The sterically encumbered TBS and TIPS trialkylsilyl functionalities, which are efficacious protecting groups in organic synthesis,[16] were chosen to sterically screen the inner sphere of the anion, to enhance solubility, and to further delocalize the negative charge via the established π-acceptor properties of silyl arene substituents.[17] Synthetically, nucleophilic substitution reactions on silicon occur readily and provide a reliable access to the silyl-functionalized fluoroarene groups. The synthetic routes to the triphenylcarbenium salts **3a**,**b** are shown in Scheme 1. Silyltetrafluorobenzenes **1a**,**b** are prepared from the reaction of the corresponding silyltriflates with LiC_6F_4H generated *in situ* from BrC_6F_4H in diethyl ether.[18] Arylation of BCl_3 with the fluroaryl lithium reagents formed *in situ*[19] from **1** yields the lithium salts of borates **2a** and **2b**, which are then converted by metathesis to triphenylcarbenium salts **3a**,**b**. Isolation of poorly soluble **2b** requires a large quantity of diethyl ether and is not a neccesary step. Alternatively, after washing with a small amount of ether, the crude mixture of **2b** + LiCl can be used directly in the next reaction with LiCl removal postponed to the subsequent step. A single-crystal structure of the anion $B(C_6F_4TBS)_4^-$ paired with the cation $[(1,2\text{-}Me_2Cp)_2ZrF]_2(\mu\text{-}F)^+$ has been obtained and will be discussed later.

B. Zirconium and Thorium Borate Complexes. Zr and Th metallocenium borate ion pairs are typically synthesized using redox reagents (e.g., Ag^+X^- and Fc^+X^-),[20] protonolytic reagents (e.g., $R_3NH^+X^-$),[4m,20,22] or alkide/hydride abstractors (e.g., $Ph_3C^+X^-$ [2i] and $B(C_6F_5)_3$[4a]). We chose the methide/hydride abstracting triphenylcarbenium salt because the product Ph_3CMe is soluble in saturated hydrocarbon solvents, hence, it is readily removed from the metallocenium product.

A series of cationic ion-paired zirconium and thorium (fluoroaryl)borate complexes (**4a**,**b**, **5a**−**c**, **7a**−**c**, and **8a**−**c**) was prepared in high yield by reaction of the corresponding neutral dimethylmetal compounds with the appropriate triphenylcarbenium borate salt in an aromatic hydrocarbon solvent at room temperature (eq 6). All of these compounds were characterized by

$$LL'MMe_2 + \mathbf{3a}\text{−}\mathbf{c} \xrightarrow[C_6H_6]{RT} \underset{\mathbf{4a},\mathbf{b},\ \mathbf{5a},\mathbf{b},\ \mathbf{7a}\text{−}\mathbf{c},\ \mathbf{8a}\text{−}\mathbf{c}}{LL'MMe^+X^-} + Ph_3CMe \quad (6)$$

3a, $Ph_3C^+B(C_6F_4TBS)_4^-$;

3b, $Ph_3C^+B(C_6F_4TIPS)_4^-$;

3c, $Ph_3C^+B(C_6F_5)_4^-$

4a, $Cp_2ZrMe^+B(C_6F_4TBS)_4^-$;

4b, $Cp_2ZrMe^+B(C_6F_4TIPS)_4^-$;

5a, $(1,2\text{-}Me_2Cp)_2ZrMe^+B(C_6F_4TBS)_4^-$;

5b, $(1,2\text{-}Me_2Cp)_2ZrMe^+B(C_6F_4TIPS)_4^-$;

7a, $[(Me_4Cp)SiMe_2(N^tBu)]ZrMe^+B(C_6F_4TBS)_4^-$;

7b, $[(Me_4Cp)SiMe_2(N^tBu)]ZrMe^+B(C_6F_4TIPS)_4^-$;

7c, $[(Me_4Cp)SiMe_2(N^tBu)]ZrMe^+B(C_6F_5)_4^-$;

8a, $(Me_5Cp)_2ThMe^+B(C_6F_4TBS)_4^-$;

8b, $(Me_5Cp)_2ThMe^+B(C_6F_4TIPS)_4^-$;

8c, $(Me_5Cp)_2ThMe^+B(C_6F_5)_4^-$

standard spectroscopic methods and analytical techniques (see Experimental Section for data). The anions $B(C_6F_4TBS)_4^-$ and $B(C_6F_4TIPS)_4^-$ were found to impart good solubilities to the ion-pairs, a property which renders characterization straightforward and the study of the ion-pair structure in solution possible. An interesting example is complex **7a**, which to our surprise, *is readily soluble in saturated hydrocarbon solvents such as pentane.* This property also unfortunately renders isolation of **7a** relatively difficult and lowers the

(16) (a) Kunz, H.; Waldmann, H. In *Comprehensive Organic Synthesis*; Trost, B. M., Fleming, I., Winterfelt, E., Eds.; Pergamon Press: Oxford, 1991; Vol. 6, pp 652−657. (b) Lalonde, M.; Chan, T. H. *Synthesis* **1985**, 817−845.

(17) (a) Zhang, S. Z.; Zhang, X. M.; Bordwell, F. G. *J. Am. Chem. Soc.* **1995**, *117*, 602−606. (b) Wetzel, D. M.; Brauman, J. I. *J. Am. Chem. Soc.* **1988**, *110*, 8333−8336. (c) Schleyer, P. von R.; Clark, T.; Kos, A. J.; Spitznagel, G. W.; Rohde, C.; Arad, D.; Houk, K. N.; Rondan, N. G. *J. Am. Chem. Soc.* **1984**, *106*, 6467−6475. (d) Hopkinson, A. C.; Lien, M. H. *J. Org. Chem.* **1981**, *46*, 998−1003.

(18) Tamborski, C.; Soloski, E. J. *J. Org. Chem.* **1966**, *31*, 743−745.

(19) (a) Massey, A. G.; Park, A. J. *J. Organomet. Chem.* **1964**, *2*, 245−250. (b) Massey, A. G.; Park, A. J. *J. Organomet. Chem.* **1966**, *5*, 218−225.

(20) Jordan, R. F.; Bajgur, C. S.; Dasher, W. E.; Rheingold, A. L. *Organometallics* **1987**, *6*, 1041−1051.

(21) (a) Shannon, R. D. *Acta Crystallogr., Sect. A* **1976**, *32*, 751−767. (b) Huheey, J. E. *Inorganic Chemistry*, 3rd ed.; Harper and Row: New York, 1983; pp 258−259.

(22) Lin, Z.; Le Marechal, J. F.; Sabat, M.; Marks, T. J. *J. Am. Chem. Soc.* **1987**, *109*, 4127−4129.

preparative yield, even though eq 6 is determined to be quantitative by ^{1}H NMR. In contrast, the $B(C_6F_5)_4^-$-derived ion pairs often have poor solubilities. Thus, solution ^{13}C NMR data for complex **8c** could not be obtained due to poor solubility in benzene. Instead, CPMAS techniques were employed to obtain the solid state ^{13}C NMR spectrum. Compound **7c** also has very limited solubility in benzene, and ^{13}C spectra could only be obtained (for nuclei with attached protons) by two-dimensional HMQC NMR techniques. Note that isolated solid complex **7c** invariably contains 1 equiv of aromatic solvent judging from NMR integration (confirmed by elemental analysis—see Experimental Section). The Zr:solvent molecule stoichiometry remains 1:1 even after prolonged pumping under high vacuum. These results suggest coordination of the arene solvent molecule to the cation (for additional discussion, see section II). A characteristic NMR spectroscopic feature of all of the methyl ion pairs is that the ^{13}C resonance of the M−Me$^+$ group is shifted considerably downfield compared to the corresponding neutral precursor M−Me$_2$ groups. The only exception is the **7c** Zr−Me signal, which is likely influenced by the diamagnetic anisotropy of the coordinated arene.

Attempts to isolate analogous cationic metallocene complexes via reaction of **3a** or **3b** with $(Me_5Cp)_2ZrMe_2$ and of **3c** with Cp_2ZrMe_2, $(1,2\text{-}Me_2Cp)_2ZrMe_2$, or $(Me_5Cp)_2ZrMe_2$ result in complicated oily mixtures of unidentified species (for discussion of the stabilities, see section IV). However, exposure of these mixtures to dihydrogen leads to cationic ion-paired hydrides (**5a**, **6a**−**c**) in high yields (eq 7). These complexes exhibit

$$L_2MMe_2 + \mathbf{3a}-\mathbf{c} \xrightarrow[-CH_4]{RT,\ 1\ atm\ H_2} \underset{\mathbf{5c},\ \mathbf{6a}-\mathbf{c}}{L_2MH^+X^-} + Ph_3CMe \qquad (7)$$

3a, $Ph_3C^+B(C_6F_4TBS)_4^-$;

3b, $Ph_3C^+B(C_6F_4TIPS)_4^-$;

3c, $Ph_3C^+B(C_6F_5)_4^-$

5c, $(1,2\text{-}Me_2Cp)_2ZrH^+B(C_6F_5)_4^-$;

6a, $(Me_5Cp)_2ZrH^+B(C_6F_4TBS)_4^-$;

6b, $(Me_5Cp)_2ZrH^+B(C_6F_4TIPS)_4^-$;

6c, $(Me_5Cp)_2ZrH^+B(C_6F_5)_4^-$

straightforward ^{1}H NMR spectra with one exception. The reaction product of **3c** with Cp_2ZrMe_2 yields an immediate precipitate upon exposure to dihydrogen; the product is insoluble in aromatic hydrocarbon solvents and only barely soluble in THF. The ^{1}H NMR spectrum of the product in THF-d_8 is too complex to assign with confidence. Compounds **6a**,**b** were characterized by standard spectroscopic methods and elemental analysis (see Experimental Section for data). Compound **5c** is insoluble in aromatic solvents, including 1,2-dichlorobenzene. The ^{1}H NMR spectrum of **5c** was recorded using THF-d_8 as the solvent, revealing features similar to those of an analogous cationic zirconium hydride **C** having two molecules of trans-coordinated PMe_3.[20] The ^{13}C NMR spectra of compounds **5c** and **6c** could not be obtained due to poor solubility. All of the above cationic zirconocene hydrides exhibit characteristic downfield-shifted ^{1}H NMR signals of the Zr−H$^+$ group, in agreement with analogous cationic metallocene hydrides.[4a,20]

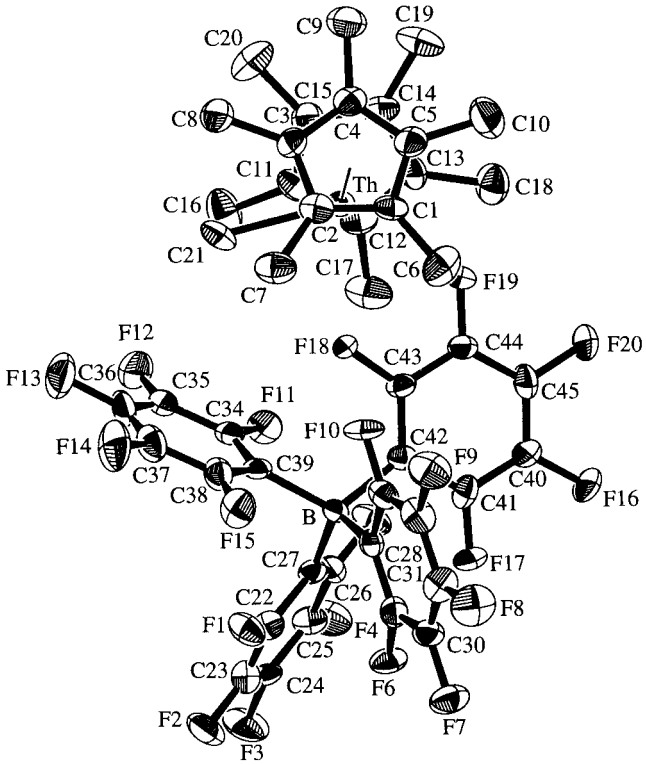

Figure 1. Perspective ORTEP drawing of the molecular structure of complex $(Me_5Cp)_2ThMe^+B(C_6F_5)_4^-$ (**8c**). Thermal ellipsoids are drawn at the 50% probability level.

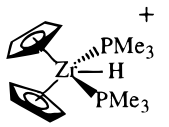

C

Numerous attempts were made during the course of this study to grow single crystals of complexes **4**−**8** suitable for X-ray analysis. However, all crystals obtained suffered from severe twinning and disorder except for **8c**, which has been crystallographically characterized. The single-crystal diffraction study of **8c** reveals a structure consisting of loosely associated $(Me_5Cp)_2ThMe^+$ cations and tetrahedral $B(C_6F_5)_4^-$ counteranions (Figure 1). Important bond distances and bond angles of **8c** derived from the final refinement are summarized in Table 2. For each molecule of **8c**, there are 2.5 solvent (benzene) molecules present in the unit cell. However, their locations rule out any direct interactions with the thorium ion.

It can be seen from Figure 1 that one aryl ring of the anion approaches the cationic metal center in the equatorial girdle plane between the two cyclopentadienyl rings, with two fluorine atoms (F18, F19) in closest proximity to the metal cation (Th−F18 = 2.757(4) Å, Th−F19 = 2.675(5) Å). These Th···F distances are considerably longer than the sums of relevant Th^{4+} and F^- ionic radii (2.28 Å)[21] and typical Th−O (THF) dative bond distances, after correcting for differences in F/O covalent radii (2.56 Å).[22] The Th···F distances in **8c** are comparable to the corresponding Zr···F(arene) distances in $(Me_5Cp)_2ZrH^+HB(C_6F_5)_3^-$ (**D**),[4a] after correcting for differences in Th/Zr ionic radii (2.64 and 2.75 Å). Furthermore, the C43−F18 and C44−F19 bond lengths in **8c** (1.325(6) and 1.344(7) Å, respectively) are slightly greater or indistinguishable from the average C−F bond length in the $B(C_6F_5)_4^-$ anion (1.32 Å). However, the

Table 2. Selected Bond Lengths (Å) and Angles (deg) for Complex 8c

Bond Lengths			
Th−C1	2.725(8)	F3−C24	1.346(9)
Th−C2	2.774(7)	F4−C25	1.318(6)
Th−C3	2.766(8)	F5−C26	1.305(9)
Th−C4	2.729(8)	F6−C29	1.306(7)
Th−C5	2.728(8)	F7−C30	1.326(8)
Th−C11	2.791(8)	F8−C31	1.353(6)
Th−C12	2.762(8)	F9−C32	1.330(7)
Th−C13	2.757(8)	F10−C33	1.305(7)
Th−C14	2.761(8)	F11−C34	1.312(7)
Th−C15	2.751(8)	F12−C35	1.349(7)
Th−C21	2.399(8)	F13−C36	1.350(7)
Th−F18	2.757(4)	F14−C37	1.311(8)
Th−F19	2.675(5)	F15−C38	1.296(7)
B−C27	1.70(1)	F16−C40	1.319(7)
B−C28	1.68(1)	F17−C41	1.281(7)
B−C39	1.70(1)	F18−C43	1.325(6)
B−C42	1.70(1)	F19−C44	1.344(7)
F1−C22	1.294(6)	F20−C45	1.358(7)
F2−C23	1.332(9)		
F3−C24	1.346(9)		
Bond Angles			
Th−C1−C6	119.3(5)	Th−C14−C19	123.4(5)
Th−C2−C7	119.0(6)	Th−C15−C20	120.7(6)
Th−C3−C8	121.7(5)	C27−B−C28	115.1(6)
Th−C4−C9	124.3(5)	C27−B−C42	113.4(6)
Th−C5−C10	116.8(5)	C27−B−C39	100.9(6)
Th−C11−C16	124.1(6)	C28−B−C42	100.0(6)
Th−C12−C17	119.5(6)	C28−B−C39	113.7(6)
Th−C13−C18	120.5(5)	C39−B−C42	114.4(6)
$Cp_{ring-centroid}-Th-Cp_{ring-centroid}$			140.1(3)

corresponding C−F bond lengths in **D** (1.379(6) and 1.396(5) Å) are conspicuously greater than the average C−F bond distance (1.35 Å) in the $HB(C_6F_5)_3^-$ anion of **D**. All other C−F distances in **8c** and **D** are unexceptional when compared to a typical $C(sp^2)-F$ σ-bond in other organofluorine molecules.[23] These data clearly show that despite the strong Lewis acidity of the Th cation, the cation−anion coordinative interaction is rather weak, in agreement with NMR observations in solution (*vide infra*). In addition, the cation−anion interaction in **8c** appears to be somewhat weaker than that in **D**, judging from the fact that the anion structure is less perturbed (also in agreement with solution NMR results[4a]).

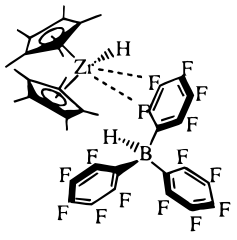

D

The $(Me_5Cp)_2ThMe^+$ cation of **8c** adapts the usual bent-sandwich configuration, and the ring centroid−Th−ring centroid angle (149.1(3)°) is not unusual for complexes containing $(Me_5Cp)_2M$ (M = lanthanide, actinide, or group 4 metals) moities.[4ac,24] However, the Th−Me and $Th-C_{ring}$(av) distances in **8c** (2.399(8) and 2.754 Å, respectively) are significantly *shorter* than those found in analogous thorium cationic complexes containing other counterions and/or Lewis bases (in $(Me_5Cp)_2ThMe(THF)_2^+$, Th−Me = 2.49(1) Å, $Th-C_{ring}$(av) = 2.80 Å;[21] in $(Me_5Cp)_2ThMe(THF)^+$, Th−Me = 2.433(7) Å, $Th-C_{ring}$(av) = 2.763 Å;[4c] in $[(Me_5Cp)_2ThMe^+]_2Fe(B_9C_2H_{11})_2^{2-}$, Th−Me = 2.480(3) Å, $Th-C_{ring}$(av) = 2.817 Å[4e]). Such shortening of the Th−Me and $Th-C_{ring}$(av) contacts doubtless reflects increased electron deficiency and coordinative unsaturation at the metal center.

II. Ion-Paired Alkyl- and Hydridozirconium and Alkylthorium (Fluoroaryl)borate Complexes. Coordination of Anions, Neutral Metal Dialkyls, and Solvents. Due to the high Lewis acidity of the cationic species, weak occupancy of the open coordination site at the metal center normally occurs and logically affects the catalytic performance of these highly unsaturated complexes.[3,4] Three types of common coordination will be discussed: anion coordination, neutral metal alkyl coordination, and solvent coordination.

Anion Coordination. In nonpolar hydrocarbon solvents such as toluene, which are commonly used for olefin polymerization, the cation−anion interaction is doubtless an important modulator of reactivity in this class of ion-paired complexes.[4] Hence, assessing the coordinative ability of the present noncoordinating anions in this type of cationic, unsaturated environment is of great interest. Evaluation of the relative coordinative ability of the anions $B(C_6F_4TBS)_4^-$, $B(C_6F_4TIPS)_4^-$, $B(C_6F_5)_4^-$, and $Me(C_6F_5)_3^-$ was probed by measuring the energetics of dynamic solution structural reorganization processes by NMR.

A unique molecular dynamic process observable in $(1,2\text{-}Me_2Cp)_2ZrMe^+X^-$ complexes is ion pair reorganization/symmetrization of the disymmetric ground state structure indicated by permutation of the diastereotopic ring methyl groups (eq 8). It is physically reasonable

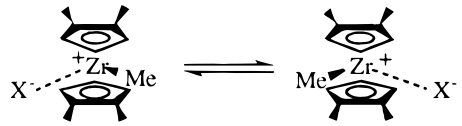

(8)

that the activation energetic parameters of such a process measure the barriers to essentially complete (or at least to the same degree) ion-pair dissociation (presumably within a solvent cage). Studies in this laboratory previously quantified these parameters by dynamic NMR techniques for $(1,2\text{-}Me_2Cp)_2ZrMe^+MeB(C_6F_5)_3^-$.[4b,f] The same measurement was performed in the present study on complexes **5a**,**b**. The rate constants for this process were determined by line shape analysis of the variable-temperature ^1H NMR spectra (Figure 2) using the appropriate modified Bloch equation.[12] The activation enthalpies and entropies (Table 3) were derived from a least-squares Eyring analysis (Figure 3) according to eq 9, where k_B is the Boltzmann constant, and h

$$\ln(k/T) = -(\Delta H^{\ddagger}/R)(1/T) + [\Delta S^{\ddagger}/R + \ln(k_B/h)] \quad (9)$$

is Planck's constant. The activation enthalpies for $(1,2\text{-}Me_2Cp)_2ZrMe^+B(C_6F_4TBS)_4^-$ (**5a**) and $(1,2\text{-}Me_2Cp)_2ZrMe^+B(C_6F_4TIPS)_4^-$ (**5b**) ion-pair reorganization are significantly lower than that for $(1,2\text{-}Me_2Cp)_2ZrMe^+MeB(C_6F_5)_3^-$, arguing that the strength of the anion coordination is less than that in $(1,2\text{-}Me_2Cp)_2ZrMe^+$-

(23) Trotter, J. In *The Chemistry of the Carbon-Halogen Bond*; Patai, S., Ed.; Wiley: London, 1973; Chapter 2.

(24) (a) Jeske, G.; Lauke, H.; Mauermann, H.; Schumann, H.; Marks, T. J. *J. Am. Chem. Soc.* **1985**, *107*, 8111−8118. (b) Schumann, H.; Meese-Marktscheffel, J. A.; Esser, L. *Chem. Rev.* **1995**, *95*, 865−986. (c) Schaverien, C. J. *Adv. Organomet. Chem.* **1994**, *36*, 283−362.

Table 3. Activation Energetic Parameters for the Ion Pair Reorganization Process in (1,2-Me$_2$Cp)$_2$ZrMe$^+$X$^-$ Complexes

X$^-$	$\Delta H^{\ddagger}$, kcal/mol	$\Delta S^{\ddagger}$, eu	$\Delta G_{coal}^{\ddagger}$, kcal/mol[a]	T_c (coalescence temperature), °C	ref
MeB(C$_6$F$_5$)$_3^-$	24(1)	17(2)	18.3(2)	80(1)	4b
B(C$_6$F$_4$TBS)$_4^-$	18.6(8)	11(1)	15(1)	56(1)	this work
B(C$_6$F$_4$TIPS)$_4^-$	19.2(4)	10(1)	15.8(7)	65(1)	this work

[a] $\Delta G_{coal}^{\ddagger}$ at the coalecence temperature.

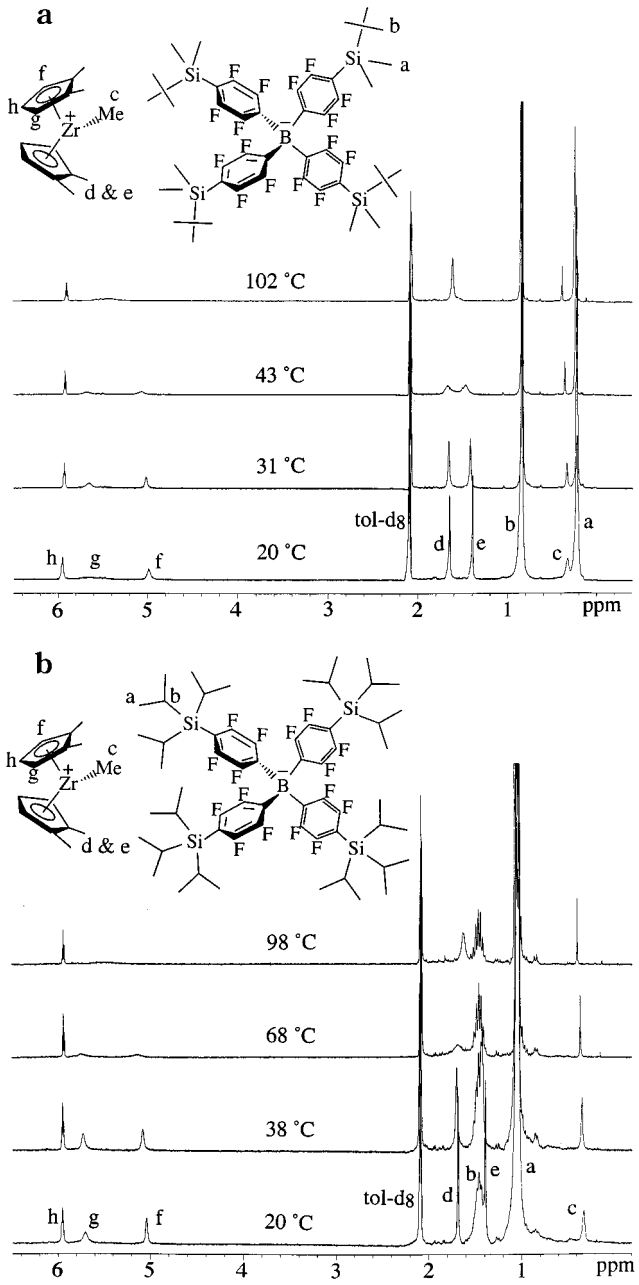

Figure 2. (a) Variable temperature ^{1}H NMR spectra of complex **5a** in toluene-d_8 solution. (b) Variable temperature ^{1}H NMR spectra of complex **5b** in toluene-d_8 solution. The ^{1}H signal line broadening of the two diastereotopic cyclopentadienyl methyl groups (H$_d$ and H$_e$, δ 1.61 and 1.37 ppm in **5a**, δ 1.73 and 1.43 ppm in **5b**) is measured as a function of temperature. These spectra also illustrate the high thermal stability of these complexes.

MeB(C$_6$F$_5$)$_3^-$ (Table 3). The activation entropies for **5a**,**b** are also somewhat lower (Table 3), possibly reflecting less ordered ground states in the more loosely associated ion pairs of **5a**,**b**. On the basis of these results, it is clear that MeB(C$_6$F$_5$)$_3^-$ associates more

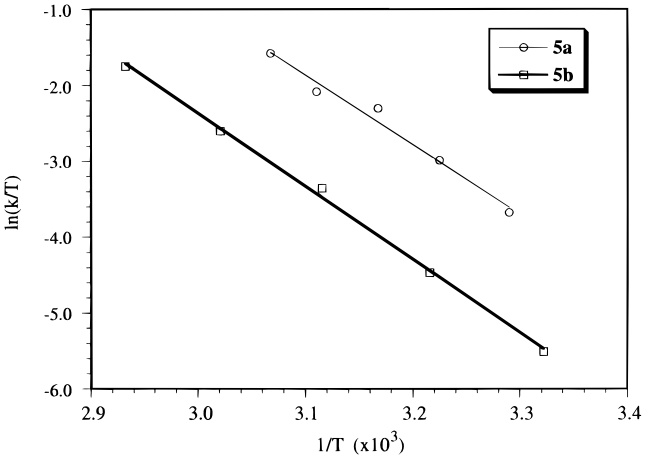

Figure 3. Eyring plot for solution dynamic ion pair reorganization processes in complexes **5a** and **5b**.

tightly with (1,2-Me$_2$Cp)$_2$ZrMe$^+$ than do B(C$_6$F$_4$TBS)$_4^-$ and B(C$_6$F$_4$TIPS)$_4^-$. This comparison is likely to be valid for the ion-pairing in complexes of the other cations discussed in this work, as will be argued below.

The ^{19}F NMR chemical shift positions and line shapes within the fluoroaryl groups are affected little by the coordination in the MeB(C$_6$F$_5$)$_3^-$-derived ion-paired L$_2$ZrMe$^+$ complexes since the cation−anion interaction is largely through a Zr$^+$−Me−B$^-$ contact (**E**).[4a] However,

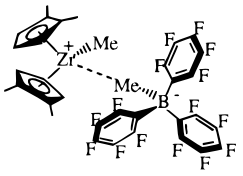

E

interactions between the cations and B(C$_6$F$_4$TBS)$_4^-$, B(C$_6$F$_4$TIPS)$_4^-$, and B(C$_6$F$_5$)$_4^-$ significantly influence the borate ^{19}F NMR spectra, which is presumably a consequence of direct metal−fluorine interactions. Comparison of the ^{19}F NMR spectra of ion-paired (fluoroaryl)borate anions to those of the corresponding triphenylcarbenium borates, in which the carbocations adopt a planar trigonal geometry and do not interact significantly with the anion,[25] provides useful information about the cation−anion interaction. In the (Me$_5$Cp)$_2$ThMe$^+$ system, the fact that the ^{19}F NMR spectrum of **8c** shows no substantial chemical shift differences from that of Ph$_3$C$^+$B(C$_6$F$_5$)$_4^-$ at room temperature suggests that coordination of anion B(C$_6$F$_5$)$_4^-$ to Th is weak and labile. In fact, only minor line broadening of the three ^{19}F signals in **8c** is observed at temperatures as low as −80 °C. In contrast, the interaction of anions

(25) (a) Nenitzescu, C. D. In *Carbonium Ions*; Olah, G. A., Schleyer, P. von R., Eds.; Wiley: New York, 1968, Vol. 1, pp 2−7. (b) For a crystal structure of a trityl salt with the counteranion perfluorobis(4,4′-biphenyl)borate, see: Ishihara, A.; Marks, T. J. Manuscript in preparation.

$B(C_6F_4TBS)_4^-$ and $B(C_6F_4TIPS)_4^-$ with Th appears to be relatively strong and causes severe line broadening of the ^{19}F signals at room temperature, due to relatively slow permutation of the fluoroaryl groups. In the $(Me_5Cp)_2ZrH^+$ system, ^{19}F line broadening of all three anions, $B(C_6F_4TBS)_4^-$, $B(C_6F_4TIPS)_4^-$, and $B(C_6F_5)_4^-$, is observed at room temperature; however, $B(C_6F_4TBS)_4^-$ and $B(C_6F_4TIPS)_4^-$ are affected more than $B(C_6F_5)_4^-$ judging from the absolute line widths at half-height of the signals corresponding to ortho and meta fluorines. The anion coordination is also strong in $[(Me_4Cp)SiMe_2(N^tBu)]ZrMe^+$ $B(C_6F_4TBS)_4^-$ (**7a**) and $[(Me_4Cp)SiMe_2(N^tBu)]ZrMe^+B(C_6F_4TIPS)_4^-$ (**7b**), judging from the room temperature ^{19}F spectrum of **7a** which exhibits a very broad envelope and that of **7b** which exhibits two sharp peaks on top of a broad envelope. In sharp contrast, the cation−anion interaction in $[(Me_4Cp)SiMe_2(N^tBu)]ZrMe(C_6H_6)^+B(C_6F_5)_4^-$ (**7c**) is replaced by coordination of an aromatic solvent molecule (*vide infra*) and the ^{19}F NMR spectrum is identical to that of the free anion even at −17 °C (very dilute solution; spectra at still lower temperatures could not be obtained due to solubility limitations), indicating the absence of significant cation−anion interactions. Interestingly, the ^{19}F spectra of the ion pairs **5a**,**b**, **6a**,**b**, **7a**,**b**, and **8a** proceed through a similar series of complicated signal broadening and sharpening on lowering the temperature in toluene-d_8 from room temperature to −90 °C. In all cases, the slow exchange limit spectra exhibit similar complex patterns with 12 signals from δ −115 to −155 ppm, having nonequivalent intensities, suggesting similar contact ion-pairing modes in the static structures. In addition, complex **7a** is soluble in pentane, suggesting a tightly associated ion pair, and ^1H NMR signal line broadening corresponding to the hypothetical dynamic process of eq 10 is not observed in toluene-d_8 at temperatures as high as 120 °C/400 MHz.

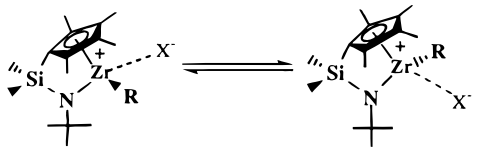

(10)

Taken together, the spectroscopic information argues that $B(C_6F_4TBS)_4^-$ and $B(C_6F_4TIPS)_4^-$ coordinate more strongly than $B(C_6F_5)_4^-$, although it does not differentiate among the steric and dative aspects of the interactions.

On the basis of these observations, the approximate relative coordinating abilities of the (fluoroaryl)borate anions with respect to the present metallocene cations can be ranked as $MeB(C_6F_5)_3^-$ > $B(C_6F_4TBS)_4^-$ ≈ $B(C_6F_4TIPS)_4^-$ > $B(C_6F_5)_4^-$. Interestingly, a correlation is also seen between this ranking and the ^{13}C chemical shifts of the $M-Me^+$ groups. That is, the weaker the anionic donor, the further downfield the signal is displaced (Table 4), presumably also, among other factors, reflecting the progression in the electron-difficiency/cationic character of the metal centers. Solvent coordination and neutral metal alkyl coordination will be discussed below. Both of these phenomena offer further supporting information for evaluating relative anions coordinative abilities.

Neutral Metallocene Alkyl Coordination. Coordination of neutral metal alkyl compounds to the cationic species results in μ-Me-bridged bimetallic complexes (eq 11). These compounds are usually much less

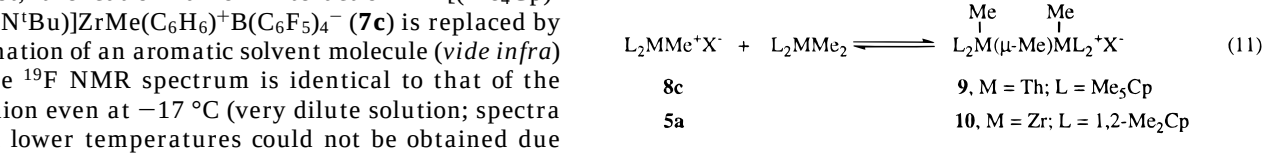

(11)

soluble than the corresponding neutral and ion-paired compounds, a property that can be utilized in their syntheses. Compound **9** is isolated as a crystalline precipitate when $(Me_5Cp)_2ThMe^+B(C_6F_5)_4^-$ (**8c**) and $(Me_5Cp)_2ThMe_2$ are mixed in benzene. The zirconocene analogue of **9** was proposed by Bochmann *et al*. on the basis of NMR studies but was not isolated in a pure state.[26] We also find that reaction of $(1,2\text{-}Me_2Cp)_2ZrMe^+B(C_6F_4TBS)_4^-$ (**5a**) with a stoichiometric excess of $(1,2\text{-}Me_2Cp)_2ZrMe_2$ affords crystalline complex **10** in benzene. Structurally diagnostic spectral characteristics of **9** and **10** are the large $^{13}C-^1H$ coupling constants of the μ-Me functionality (130.1 and 132.8 Hz, respectively).[26−28] In both cases, the ^{19}F NMR spectra of the bimetallic compounds are identical to those of the corresponding trityl salt, indicating a weak cation−anion interaction in solution. Unlike **9**, which is stable in benzene, redissolving **10** in benzene-d_6 leads instantaneously to partial dissociation of the bimetallic species, and precursors **5a** and $(1,2\text{-}Me_2Cp)ZrMe_2$ are detected coexisting with **9**. The equilibrium constant for eq 11 is determined to be $6.3(3) \times 10^2$ L/mol at 19 °C over an 8-fold concentration range, corresponding to $\Delta G = -3.7(1)$ kcal/mol. When 1,2-dichlorobenzene-d_4 is used as the solvent, the equilibrium is shifted dramatically to the right, rendering the species on the left side of the equation undetectable. The shift of the equilibrium is apparently due to the ability of the more polar 1,2-dichlorobenzene-d_4 to stabilize the more charge-separated structure. In addition, the bridging and terminal methyl groups of complex **9** are in rapid exchange on the ^1H NMR time scale at room temperature, but can be resolved below −27 °C. However, the corresponding groups are in slow exchange in complex

Table 4. Selected $Zr-CH_3$ ^{13}C NMR Chemical Shift Data for Zirconium and Thorium Metallocenes

complex	δ, ppm	ref
$(1,2\text{-}Me_2Cp)_2ZrMe_2$	38.4[a]	9
$(1,2\text{-}Me_2Cp)_2ZrMe(THF)^+B(C_6F_4TBS)_4^-$	42.3[a]	this work
$(1,2\text{-}Me_2Cp)_2ZrMe^+MeB(C_6F_5)_3^-$	44.6[a]	4a
$(1,2\text{-}Me_2Cp)_2ZrMe^+B(C_6F_4TBS)_4^-$	45.9[a]	this work
$(1,2\text{-}Me_2Cp)_2ZrMe^+B(C_6F_4TIPS)_4^-$	47.0[a]	this work
$(Me_5Cp)_2ThMe_2$	68.5[a]	6
$(Me_5Cp)_2ThMe^+B(C_6H_5)_4^-$	71.8[a]	22
$(Me_5Cp)_2ThMe^+B(C_6F_4TBS)_4^-$	77.0[a]	this work
$(Me_5Cp)_2ThMe^+B(C_6F_4TIPS)_4^-$	77.4[a]	this work
$(Me_5Cp)_2ThMe^+B(C_6F_5)_4^-$	78[b]	this work
$(Me_5Cp)_2ThMe^+\{[(C_6F_5)_2B]_2CH^tBu\}(\mu\text{-}H)^-$	80[b]	4c

[a] In C_6D_6, 20 °C. [b] CPMAS solid state NMR, 20 °C.

(26) (a) Bochmann, M.; Lancaster, S. J. *Angew. Chem., Int. Ed. Engl.* **1994**, *33*, 1634−1637. (b) See also: Turner, H. W.; Hlatky, G. G.; Eckman, R. R. U.S. Patent 5,470,927, 1995.

(27) (a) Stern, D.; Sabat, M.; Marks, T. J. *J. Am. Chem. Soc.* **1990**, *112*, 9558−9575. (b) Evans, W. J.; Chamberlain, L. R.; Ulibarri, T. A.; Ziller, J. W. *J. Am. Chem. Soc.* **1988**, *110*, 6423−6432. (c) Busch, M. A.; Harlow, R.; Watson, P. L. *Inorg. Chim. Acta* **1987**, *140*, 15−20. (d) Holton, J.; Lappert, M. F.; Pearce, R.; Yarrow, P. I. W. *Chem. Rev.* **1983**, *83*, 135−201.

(28) Ozawa, F.; Park, J. W.; Mackenzie, P. B.; Schaefer, W. P.; Henling, L. M.; Grubbs, R. H. *J. Am. Chem. Soc.* **1989**, *111*, 1319−1327.

10 at room temperature. This difference presumably reflects the larger ionic radius of Th^{4+}, which renders the transition state for methyl group permutation sterically more accessible.

When the (fluoroaryl)borate counteranions are varied, a drastically different behavior than that observed between **5a** or **8c** and the corresponding neutral metallocene dialkyls is observed. In contrast to **8c**, $(Me_5Cp)_2ThMe^+B(C_6F_4TBS)_4^-$ (**8a**) and $(Me_5Cp)_2ThMe^+B(C_6F_4TIPS)_4^-$ (**8b**) *do not* form ^1H NMR-detectable bimetallic species with $(Me_5Cp)_5ThMe_2$ in benzene. However, when **8a** and **8b** are mixed with $(Me_5Cp)_5Th(^{13}CH_3)_2$ in C_6D_6, rapid (within 1 h) ^{13}C isotopic scrambling is observed between cationic and neutral Th species, suggesting that eq 9 is operative but lies further to the left in both cases. Unlike **5a**, $(1,2\text{-}Me_2Cp)_2ZrMe^+MeB(C_6F_5)_3^-$ does not form a detectable bimetallic species with $(1,2\text{-}Me_2Cp)_2ZrMe_2$. Although similar isotopic scrambling is observed upon mixing $(1,2\text{-}Me_2Cp)_2Zr(^{13}CH_3)_2$ and $(1,2\text{-}Me_2Cp)_2ZrMe^+MeB(C_6F_5)_3^-$, a different mechanism involving methide abstraction to form the neutral borane may be operative in this case[4a,b] and is beyond the scope of this discussion. These results, as well as those in eq 11, can be explained in terms of competition between the (fluoroaryl)borate anions and the neutral metal alkyls for the metallocene cations. For $(1,2\text{-}Me_2Cp)_2ZrMe^+$ paired with counteranion $MeB(C_6F_5)_3^-$, anion coordination is stronger than binding of $(1,2\text{-}Me_2Cp)_2ZrMe_2$ and a μ-Me bimetallic complex is not detected. However, when $B(C_6F_4TBS)_4^-$ is the counteranion, the coordinating strength of the anion and the binding of $(1,2\text{-}Me_2Cp)_2ZrMe_2$ are comparable and **9** is in equilibrium with **5a** and $(1,2\text{-}Me_2Cp)_2ZrMe_2$. For $(Me_5Cp)_2ThMe^+$ paired with $B(C_6F_5)_4^-$, anion coordination is much weaker than that of $(Me_5Cp)_2ThMe_2$ and sizable concentrations of the bimetallic species are present in benzene solution. In contrast, when $B(C_6F_4TBS)_4^-$ is the counteranion, anion coordination is stronger than that of $(Me_5Cp)_2ThMe_2$ and detectable quantities of a μ-Me bimetallic complex are not formed. These observations demonstrate again that relative coordination ability follows the order $MeB(C_6F_5)_3^- > B(C_6F_4TBS)_4^- \approx B(C_6F_4TIPS)_4^- > B(C_6F_5)_4^-$. NMR scale reactions of either **7a** or **7c** with the corresponding neutral precursors gave no evidence of dimeric μ-Me species.

Solvent Coordination. Although significant coordination of arene ligands to cationic metallocene species has not been observed, it is an important interaction in complexes such as $(Me_5Cp)ZrMe_2^+MeB(C_6F_5)_3^-$, which exists as a toluene adduct both in solution and in the solid state.[29] In the present study, arene coordination to the constrained geometry Zr cation $[(Me_4Cp)SiMe_2(N^tBu)]ZrMe^+$ is observed when the counteranion is $B(C_6F_5)_4^-$, as noted in section II. In addition to the analytical evidence already presented, other spectroscopic evidence also supports the coordination of arenes to this type of ion pair. The ^{19}F spectrum of **7c** in toluene-d_8 displays three sharp peaks in the fluoroaromatic region with coupling constants and chemical shifts identical to those of the free anion in $Ph_3C^+B(C_6F_4)_4^-$, consistent with the absence of significant cation−anion interaction. The ^1H spectrum of **7c** in toluene-d_8 indicates nonlabile occupancy of the coordination site on Zr adjacent to the methyl group, as significant line broadening of the diastereotopic Cp and silyl methyl groups is not observed at temperatures below 80 °C. At temperatures above 80 °C, broadening of the diastereotopic methyl signals is observed, presumably resulting from dynamic symmetrization processes (e.g., eq 12, possibly assisted by other solvent molecules). At still

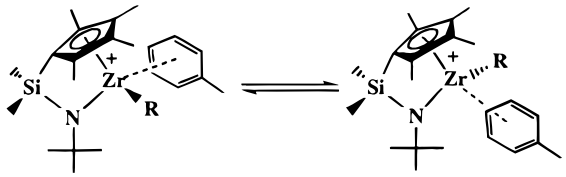

(12)

higher temperatures, irreversible decomposition occurs, rendering it difficult to accurately determine the rate of the dynamic process. The rate can be roughly estimated as $\sim 62\ s^{-1}$ at the coalescence temperature (94 °C)[12] of one set of diastereotopic cyclopentadienyl methyl groups, corresponding to $\Delta G^{\ddagger} \approx 24.9$ kcal/mol. In addition, the Zr^+-Me group ^1H NMR signal (δ −0.45 ppm) and ^{13}C signal (δ 32.2 ppm) in $[(Me_4Cp)SiMe_2(N^tBu)]_2ZrMe(C_6H_6)^+B(C_6F_5)_4^-$ (**7c**) are at a surprisingly high field compared to the other cationic group 4 and Th complexes (Table 4), all of which have low field M^+-Me resonances. Especially relevent are analogous complexes **7a** (^1H, δ 0.21 ppm; ^{13}C, δ 56.9 ppm) and **7b** (^1H, δ 0.23 ppm; ^{13}C, δ 57.2 ppm). Such a dramatic chemical shift difference is reasonably ascribed to the diamagnetic anisotropy of the coordinated arene ring.

Thermal Stability. Good stability at high temperatures (e.g., ≥100 °C) is a crucial prerequisite for the application of metallocene complexes in industrial scale olefin polymerization technologies. We previously studied the thermal decomposition of $MeB(C_6F_5)_3^-$-based cationic metallocene complexes and identified four major thermal decomposition pathways in toluene-d_8 (cation/anion ligand redistribution, intramolecular C−H activation, fluoride abstraction, and intermolecular C−H activation).[4a] The thermal stability of the ion-paired complexes was found to be a sensitive function of the cyclopentadienyl ancillary ligand subtituents. In the present investigation, the roles of both the ancillary ligand and the counteranion in stabilizing the cations were studied. The zirconocene complexes with unsubstituted cyclopentadienyl ligands (**4a**,**b**) and the $(Me_5Cp)_2Th$ complexes (**8a**−**c**) exhibit moderate thermal stability at room temperature and decompose rapidly at 70−80 °C in benzene. In the case of **4a**, the major thermolysis pathway is aryl group redistribution between cation and anion (eq 13), resulting in a neutral metallocene compound, which can be crystallized from the reaction mixture at −78 °C .[30] The other decom-

$$Cp_2ZrMe^+B(C_6F_4TBS)_4^- \xrightarrow[\text{toluene}]{70-80\ ^\circ C} Cp_2ZrMe(C_6F_4TBS) + B(C_6F_4TBS)_3 \quad (13)$$

position product in this case is presumably a neutral

(29) (a) Gillis, D. J.; Tudoret, M.-J.; Baird, M. C. *J. Am. Chem. Soc.* **1993**, *115*, 2543−2545. (b) Lancaster, S. J.; Robinson, O. B.; Bochmann, M.; Coles, S. J.; Hursthouse, M. B. *Organometallics* **1995**, *14*, 2456−2462.

(30) NMR spectroscopic characterization: ^1H NMR (C_6D_6, 25 °C): δ 0.19 (t, $J_{H-F} = 4.2$ Hz, 3H, Zr−Me), 0.35 (s, 6H, Si−Me), 0.91 (s, 9H, Si−CMe_3), 5.85 (s, 10H, Cp). ^{19}F NMR (C_6D_6, 60 °C): δ −128.2 (m, 2F, C_6F_4), −132.6 (m, 2F, C_6F_4).

borane , which was not characterized in detail. Such aryl abstraction processes from borate anions by cationic Zr species have been previously reported by serveral groups.[4a,31] The other $B(C_6F_4TBS)_4^-$-, $B(C_6F_4TIPS)_4^-$-, and $B(C_6F_5)_4^-$-based Zr complexes (**5**, **6**, and **7a**−**c**) exhibit greater thermal stability than the $MeB(C_6F_5)_3^-$-based analogues and are generally stable in toluene at 100−110 °C for at least 1 h without significant decomposition. However, complex **7c** decomposes rapidly at 100 °C in toluene. After prolonged heating, the decomposition products in this case are complex mixtures that could not be unambiguously characterized.

It is interesting that the cationic methylzirconocenes having $B(C_6F_5)_4^-$ as the charge-compensating anion are not isolable at room temperature. In contrast, hydrides $(Me_5Cp)_2ZrH^+B(C_6F_5)_4^-$ (**5c**) and $(1,2\text{-}Me_2Cp)_2ZrH^+B(C_6F_5)_4^-$ (**6c**), prepared by exposing the mixtures derived from attempted syntheses of the cationic methyl complexes to H_2, exhibit good thermal stability at 100 °C. One reasonable explanation is that C−H activation processes involving the cyclopentadienyl ligand and Zr^+−Me fragment intervene to afford η^5,η^1 complexes and that the (fluoroaryl)borate anion is not directly involved. Such a process appears more likely if the cation is extremely electron-deficient and may, in principle, be avoidable if the cation is less unsaturated. In other words, a certain degree of weak coordination is required to prevent the cation from undergoing self-decomposition. In accordance with this hypothesis, the $MeB(C_6F_5)_3^-$ anion, which is the most coordinating anion identified in this work, stabilizes all four of the methylzirconium cations discussed here. However, $(1,3\text{-}^tBu_2Cp)_2ZrMe^+$, in which the highly congested ligand environment may weaken $MeB(C_6F_5)_3^-$ coordination and in which a proximate C−H functionality is present, undergoes clean ^{t}BuC−H metallation to afford an η^5,η^1 "tuck-in" cation (eq 14), which is inert with respect to ethylene polymerization or oligomerization.[4a] In comparison, the anions $B(C_6F_4TBS)_4^-$ and $B(C_6F_4TIPS)_4^-$ stabilize three of the four methylzirconium cations but do not stabilize the *sterically most hindered* $(Me_5Cp)_2ZrMe^+$. Intramolecular C−H activation and other decomposition processes are also likely to be detrimental to catalytic activity (the polymerization activity of $B(C_6F_5)_4^-$-derived catalysts erodes significantly upon storage at room temperature, *vide infra*) since the constrained geometries of the η^5,η^1 compounds may not support rapid multiple C=C insertions.[4a]

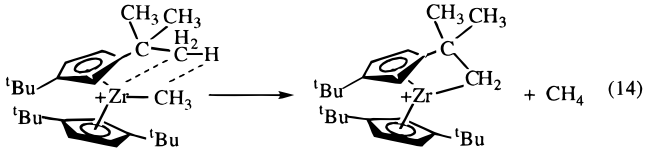

(14)

Upon prolonged standing at 25 °C over the course of several weeks, a solution of **5a** in toluene decomposed to yield single crystals of $[(1,2\text{-}Me_2Cp)_2ZrF]_2(\mu\text{-}F)^+B(C_6F_4TBS)_4^-$ (**11**), which were characterized by X-ray diffraction. Unlike previously reported $[(1,2\text{-}Me_2Cp)_2ZrMe]_2(\mu\text{-}F)^+MeB(C_6F_5)_3^-$ (also a decomposition product),[4a] the methyl groups connected to Zr are completely replaced by F in this case. The crystal structure of **11** consists of separated, discrete $[(1,2\text{-}Me_2Cp)_2ZrF]_2(\mu\text{-}F)^+$ cations and $B(C_6F_4TBS)_4^-$ anions (Figure 4). Important bond distances and bond angles of **11** are summarized in Table 5. Unlike previously characterized $[(1,2\text{-}Me_2Cp)_2ZrMe]_2(\mu\text{-}F)^+$, which has a linear Zr−F−Zr configuration, the present Zr1−F1−Zr2 angle is 159.0(6)°. The Zr−(μ-F) distances in **11** are approximately the same as those in $[(1,2\text{-}Me_2Cp)_2ZrMe]_2(\mu\text{-}F)^+$ (Zr1−F1 = 2.11(1) Å and Zr2−F1 = 2.11(1) Å *vs* 2.108(2) and 2.118(2) Å in the latter). The present terminal Zr−F bond lengths (Zr1−F3 = 1.92(1) Å and Zr2−F2 = 1.94(1) Å) are shorter than those in Cp_2ZrF_2 (1.98(1) Å),[30] presumably reflecting the electron-deficient cationic character of **11**. The two $(1,2\text{-}Me_2Cp)_2ZrF$ fragments in **11** are crystallographically nearly identical (e.g., Zr1−C_{ring}(av) = 2.51 Å and Zr2−C_{ring}(av) = 2.49 Å). The large borate anion adopts a normal tetrahedral geometry, and within the accuracy of the present determination, the average B−C(aryl) distance in **11** is comparable to or slightly shorter than the corresponding average bond distance in **8c**. The C−F distances in the four silyl-functionalized fluoroaryl ligand are unexceptional C(sp^2)−F distances.[23]

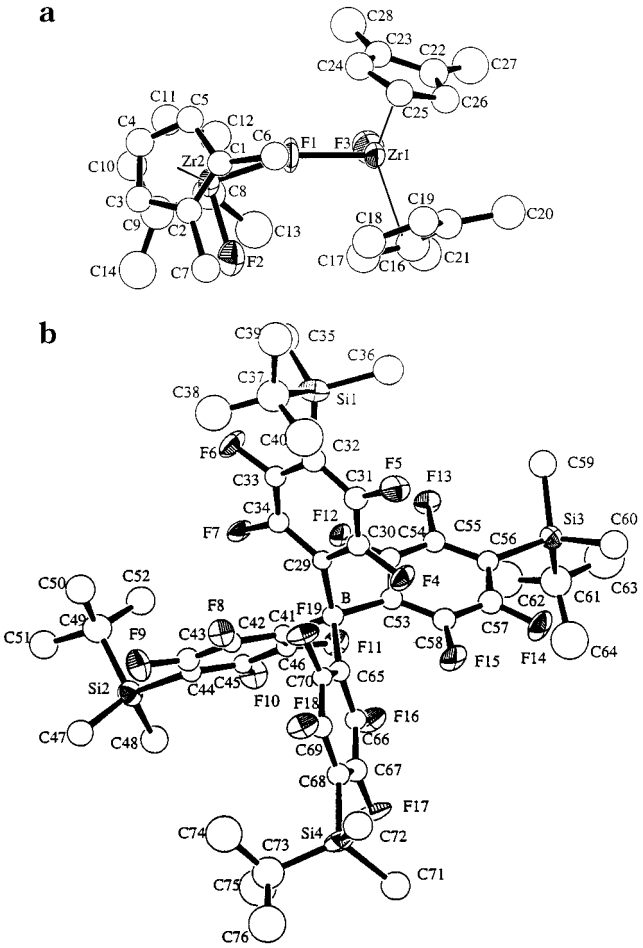

Figure 4. Perspective ORTEP drawing of the molecular structure of complex $[(1,2\text{-}Me_2Cp)_2ZrF]_2(\mu\text{-}F)^+B(C_6F_4TBS)_3^-$ (**11**). Thermal ellipsoids are drawn at the 35% probability level: (a) cation, (b) anion.

In summary, the identified metallocenium fluoroborate decomposition pathways can be divided into two categories: (i) decompositions involving the anions, e.g., the aryl transfer reactions such as eq 13 and fluoride

(31) (a) Horton, A. D.; Orpen, A. G. *Organometallics* **1991**, *10*, 3910−3918. (b) Bochmann, M.; Jaggar, A. J.; Nicholls, J. C. *Angew. Chem., Int. Ed. Engl.* **1990**, *29*, 780−781. (c) Lin, Z. Ph.D. Dissertation, Northwestern University, Evanston, IL, 1988.

(32) Bush, M. A.; Sim, G. A. *J. Chem. Soc. A* **1971**, 2225−2229.

Table 5. Selected Bond Lengths (Å) and Angles (deg) for 11

Bond Lengths			
Zr1−F1	2.11(1)	F4−C30	1.37(2)
Zr1−F3	1.92(1)	F5−C31	1.33(2)
Zr2−F1	2.11(1)	F6−C33	1.36(2)
Zr2−F2	1.94(1)	F7−C34	1.34(2)
Zr1−C15	2.48(2)	F8−C42	1.37(2)
Zr1−C16	2.55(2)	F9−C44	1.37(2)
Zr1−C17	2.51(2)	F10−C45	1.38(2)
Zr1−C18	2.46(2)	F11−C46	1.38(2)
Zr1−C19	2.49(2)	F12−C54	1.36(2)
Zr1−C22	2.53(2)	F13−C55	1.36(2)
Zr1−C23	2.51(2)	F14−C57	1.37(2)
Zr1−C24	2.50(2)	F15−C58	1.35(2)
Zr1−C25	2.48(2)	F16−C66	1.33(2)
Zr1−C26	2.44(2)	F17−C67	1.34(2)
Zr2−C1	2.56(2)	F18−C69	1.35(2)
Zr2−C2	2.54(2)	F19−C70	1.35(2)
Zr2−C3	2.48(2)	B−C29	1.66(3)
Zr2−C4	2.48(2)	B−C44	1.66(2)
Zr2−C5	2.51(2)	B−C53	1.67(3)
Zr2−C8	2.50(2)	B−C65	1.66(3)
Zr2−C9	2.55(2)	Si1−C32	1.91(2)
Zr2−C10	2.49(2)	Si2−C44	1.89(2)
Zr2−C11	2.47(2)	Si3−C56	1.90(2)
Zr1−C12	2.54(2)	Si4−C68	1.90(2)
Bond Angles			
F1−Zr2−F2	119.3(5)	C65−B−C53	113(1)
F1−Zr1−F3	119.0(6)	C29−B−C41	116(1)
Zr1−F1−Zr2	158.0(6)	C29−B−C65	112(1)
C29−B−C53	100(1)	C41−B−C65	102(1)
C41−B−C53	112(1)		
$Cp_{ring-centroid}$−Zr1−$Cp_{ring-centroid}$			131(1)
$Cp_{ring-centroid}$−Zr2−$Cp_{ring-centroid}$			131(1)

abstraction and (ii) cation self-decomposition, e.g., C−H activation reactions such as eq 14.

III. Catalytic Olefin Polymerization. The results of ethylene polymerization experiments, conducted in a manner so as to minimize mass transport effects,[4a] are shown in Table 6. The results with zirconocene catalysts are first discussed, then those with thorocene and constrained geometry catalysts. The data will be analyzed with a view toward differentiating cation and anion effects on polymerization activity. The pure, isolated organometallic salts were employed in all of the experiments except those of entries 15−17, in which the unstable $B(C_6F_5)_4^-$-derived catalysts were generated *in situ* by mixing the neutral dimethylzirconocenes with $Ph_3C^+B(C_6F_5)_4^-$ in a small volume of toluene (∼2 mL). The freshly generated $B(C_6F_5)_4^-$ catalysts exhibit high activity; however, aging significantly erodes the performance (entry 20, Table 6), in agreement with the thermal stability studies (*vide supra*). In comparison to the previously reported $MeB(C_6F_5)_3^-$-derived zirconocene catalysts,[4a] the corresponding $B(C_6F_5)_4^-$-, $B(C_6F_4TBS)_4^-$-, and $B(C_6F_4TIPS)_4^-$-derived zirconocene catalysts exhibit significantly higher ethylene polymerization activities under identical reaction conditions. Although the exact quantity of active species could not be determined for the zirconocene + $Ph_3C^+B(C_6F_5)_4^-$-based catalysts (due to the thermal instability), the corresponding $B(C_6F_5)_4^-$-, $B(C_6F_4TBS)_4^-$-, and $B(C_6F_4TIPS)_4^-$-derived zirconocene catalysts have similar overall activities and the differences among them are generally within experimental error (entries 5−10 and 15−17, Table 6). However, comparison of the activity of the thorocene (**8a**−**c**) and the constrained geometry (**7a**−**c**) catalyst classes, both of which are formally more coordinatively unsaturated than the zirconocenes, reveals that the freshly prepared $B(C_6F_5)_4^-$-derived catalysts exhibit comparable or only slightly greater reactivity than the analogous $B(C_6F_4TBS)_4^-$ and $B(C_6F_4TIPS)_4^-$ catalysts (entries 11−14, 18, and 19, Table 6). Note that the $MeB(C_6F_5)_3^-$-derived constrained geometry catalyst is almost completely inactive for ethylene polymerization (entry 4, Table 6) at room temperature. The activity differences among the catalysts having identical cationic fragments and variable counterions doubtless reflects the relative coordinative abilities of the anions and tightness of the ion-pairing. In addition to the "anion effects" on the ethylene polymerization activities, the data in Table 6 also reveal noteworthy properties of the cations. Note that the

Table 6. Ethylene Polymerization Performance of Ion-Paired Cationic Group 4 and Thorium Complexes with Various Anions[a]

entry no.	cation	anion	[cat.], mM	rxn time, s	polymer yield,[b] g	activity, ×10⁶ g PE/mol of M·atm·h[c]	M_w,[d] ×10⁵	M_w/M_n[d]
1	Cp_2ZrMe^+ [e]	$MeB(C_6F_5)_3^-$	0.32	40	0.65(5)	4.5(4)	1.24	2.0
2	$(1,2\text{-}Me_2Cp)_2ZrMe^+$ [e]	$MeB(C_6F_5)_3^-$	0.22	66	1.1(1)	6.8(7)	5.21	1.4
3	$(Me_5Cp)_2ZrMe^+$ [e]	$MeB(C_6F_5)_3^-$	0.22	62	0.58(5)	3.8(4)	2.55	2.0
4	$(Me_4Cp)SiMe_2(N^tBu)ZrMe^+$	$MeB(C_6F_5)_3^-$	0.40	900	<0.01	<0.001		
5	Cp_2ZrMe^+	$B(C_6F_4TBS)_4^-$	0.14	62	1.4(1)	5.7(6)	8.78	1.72
6	Cp_2ZrMe^+	$B(C_6F_4TIPS)_4^-$	0.14	60	1.5(2)	6.2(6)	5.65	1.32
7	$(1,2\text{-}Me_2Cp)_2ZrMe^+$	$B(C_6F_4TBS)_4^-$	0.14	10	1.9(8)	50(20)	8.29	1.57
8	$(1,2\text{-}Me_2Cp)_2ZrMe^+$	$B(C_6F_4TIPS)_4^-$	0.14	10	1.6(7)	42(20)	6.02	1.99
9	$(Me_5Cp)_2ZrMe^+$	$B(C_6F_4TBS)_4^-$	0.14	20	0.9(2)	11(2)	21.6	1.99
10	$(Me_5Cp)_2ZrMe^+$	$B(C_6F_4TIPS)_4^-$	0.14	20	0.8(2)	10(2)	12.8	1.78
11	$(Me_5Cp)_2ThMe^+$	$B(C_6F_4TBS)_4^-$	0.10	600	0.91(4)	0.92(4)	3.36	2.06
12	$(Me_5Cp)_2ThMe^+$	$B(C_6F_4TIPS)_4^-$	0.10	600	0.84(8)	1.0(1)	1.70	1.7
13	$(Me_4Cp)SiMe_2(N^tBu)ZrMe^+$	$B(C_6F_4TBS)_4^-$	0.28	600	0.25(4)	0.052(9)	0.087	2.87
14	$(Me_4Cp)SiMe_2(N^tBu)ZrMe^+$	$B(C_6F_4TIPS)_4^-$	0.25	720	0.32(5)	0.060(9)	0.068	2.52
15	Cp_2ZrMe^+ [f]	$B(C_6F_5)_4^-$	0.20	60	2.1(2)	6.4(5)	9.87	1.38
16	$(1,2\text{-}Me_2Cp)_2ZrMe^+$ [f]	$B(C_6F_5)_4^-$	0.20	22	3.2(7)	28(6)	7.03	1.61
17	$(Me_5Cp)_2ZrMe^+$ [f]	$B(C_6F_5)_4^-$	0.20	20	1.1(2)	10(2)	5.32	1.66
18	$(Me_5Cp)_2ThMe^+$	$B(C_6F_5)_4^-$	0.14	60	0.78(4)	3.6(2)	0.986	1.93
19	$(Me_4Cp)SiMe_2(N^tBu)ZrMe^+$	$B(C_6F_5)_4^-$	0.23	240	1.4(1)	0.91(1)	0.090	3.13
20	$(1,2\text{-}Me_2Cp)_2ZrMe^+$ [g]	$B(C_6F_5)_4^-$	0.20	60	1.0(2)	3.1(6)		

[a] 25 °C, 1 atm of ethylene, in 100 mL of toluene. [b] Average yield of ≥3 runs; the number in parenthesis is the standard deviation in the yield. [c] The number in the parenthesis is the standard deviation in the activity. [d] By GPC, relative to polystyrene standards. [e] Data of ref 4d. [f] Catalyst generated by *in situ* reaction of the corresponding dimethylzirconocene with $Ph_3C^+B(C_6F_5)_4^-$ in toluene (2−3 mL) for 5 min. [g] Catalyst aged for 3 h at 25 °C after generation by *in situ* reaction of $(1,2\text{-}Me_2Cp)_2ZrMe_2$ with $Ph_3C^+B(C_6F_5)_4^-$ in toluene (2−3 mL).

Table 7. Propylene Polymerization Performance of Ion-Paired Cationic Group 4 Complexes with Various Anions[a]

entry no.	cation	anion	[cat.], mM	rxn time, min	polymer yield,[b] g	activity, $\times 10^5$ g PP/mol of M·atm·h[c]	M_w,[d] $\times 10^3$	M_w/M_n[d]
1	Cp_2ZrMe^+	$MeB(C_6F_5)_3^-$	0.49	60	15.5(7)	8.1(7)		
2	$(1,2\text{-}Me_2Cp)_2ZrMe^+$	$MeB(C_6F_5)_3^-$	0.49	60	5.1(5)	2.8(3)		
3	$(Me_5Cp)_2ZrMe^+$	$MeB(C_6F_5)_3^-$	0.49	60	2.3(2)	1.4(1)		
4	$(Me_4Cp)SiMe_2(N^tBu)ZrMe^+$	$MeB(C_6F_5)_3^-$	0.47	300	0	0		
5	Cp_2ZrMe^+	$B(C_6F_4TBS)_4^-$	0.38	60	11(1)	7.5(8)	3.29	1.86
6	Cp_2ZrMe^+	$B(C_6F_4TIPS)_4^-$	0.38	60	13.6(9)	9.0(6)	2.52	1.69
7	$(1,2\text{-}Me_2Cp)_2ZrMe^+$	$B(C_6F_4TBS)_4^-$	0.37	50	16.2(1)	12.9(1)	5.19	2.15
8	$(1,2\text{-}Me_2Cp)_2ZrMe^+$	$B(C_6F_4TIPS)_4^-$	0.33	50	12.0(9)	11.0(9)	6.03	2.21
9	$(Me_5Cp)_2ZrH^+$	$B(C_6F_4TBS)_4^-$	0.35	66	2.0(5)	1.3(3)	5.15	2.12
10	$(Me_5Cp)_2ZrH^+$	$B(C_6F_4TIPS)_4^-$	0.31	70	1.8(1)	1.2(1)	2.61	1.7
11	$(Me_4Cp)SiMe_2(N^tBu)ZrMe^+$	$B(C_6F_4TBS)_4^-$	35	300	1.1(1)	0.16(1)	3.59	2.16
12	$(Me_4Cp)SiMe_2(N^tBu)ZrMe^+$	$B(C_6F_4TIPS)_4^-$	63	420	2.8(2)	0.16(1)	4.28	2.72
13	Cp_2ZrMe^+ [e]	$B(C_6F_5)_4^-$	0.39	40	11.2(1)	10.8(1)	2.30	1.64
14	$(1,2\text{-}Me_2Cp)_2ZrMe^+$ [e]	$B(C_6F_5)_4^-$	0.39	40	9.9(8)	10.2(8)	7.60	2.31
15	$(Me_5Cp)_2ZrMe^+$ [e]	$B(C_6F_5)_4^-$	0.39	40	1.3(1)	1.3(1)	2.63	1.74
16	$(Me_4Cp)SiMe_2(N^tBu)ZrMe^+$	$B(C_6F_5)_4^-$	0.29	40	6.3(1)	8.2(1)	3.64	2.20

[a] 25 °C, 1 atm of propylene, in 40 mL of toluene. [b] Average yield of two runs; the number in parenthesis is the standard deviation in the yield. [c] The number in the parenthesis is the standard deviation in the activity. [d] By GPC relative to polystyrene standards. [e] Generated by *in situ* reaction of the corresponding dimethylzirconocene with $Ph_3C^+B(C_6F_5)_4^-$.

polymerization activities of the $(1,2\text{-}Me_2Cp)_2ZrMe^+$ systems exceed those of the other cationic systems having the same counteranions, with the effect most pronounced for poorly coordinating anions (e.g., entries 7, 8, and 16 *vs* 5, 6, 9, 10, 15, and 17 in Table 6). This $(1,2\text{-}Me_2Cp)_2ZrR^+$ effect has also been observed in the case of other weakly coordinating anions developed in this laboratory.[25b,33] The constrained geometry catalysts **7a**−**c** exhibit significantly lower polymerization activities than the metallocene complexes. Although this probably reflects tight cation−anion coordination in the case of **7a** and **7b** (entries 13 and 14, Table 6), it is likely an intrinsic property of the constrained geometry cation in aromatic solvents for **7c** (entry 19, Table 6) because an arene is coordinated to the cation rather than $B(C_6F_5)_4^-$ (*vide supra*). The polymeric products of the reactions were characterized using ^1H and ^{13}C NMR spectroscopy and exibit the characteristic signatures of highly linear polyethene, except those that are produced by **7a**−**c** (entries 13, 14, and 19, Table 6), which possess branching units[34] consistent with literature reports.[5h,i]

The results of propylene polymerization experiments are shown in Table 7. The activity differences among the zirconocene catalysts as a function of anion are not as dramatic as in ethylene polymerization. The intrinsic steric and electronic characteristics of the cation appear to play a more important role in monomer coordination and insertion at the catalytic center for propylene than for ethylene polymerization, and the role of the particular anion is less distinctive. However, the activity differences among the constrained geometry complexes with various anions are amplified, and strong anion effects on polymerization activity are observed (entries 4, 11, 12, and 16, Table 7). As assayed by ^1H and ^{13}C NMR,[32] the polymerization products are all highly linear atactic polypropylenes derived from regioselective 1,2-insertion. Interestingly, the Th complexes do not catalyze propylene polymerization. Instead, catalyst **8c** reacts with propylene stoichiometrically to afford an η^3-allyl complex and methane (eq 15), identical to what has been observed with analogous lanthanide complexes.[24]

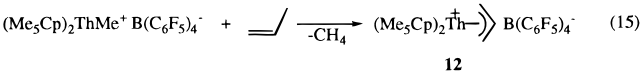

12 (15)

The present data evidence marked sensitivity of olefin polymerization rates to details of cation−anion pairing, with increased activity correlating with evidence for weakened ion-pairing. Maximum activities are observed for $B(C_6F_4TBS)_4^-$- and $B(C_6F_4TIPS)_4^-$-based pairs, with modification as $B(C_6F_5)_4^-$ not further enhancing activity and significantly eroding thermal stability. At present, the energetic profile for olefin activation and insertion in such ion-pairs has not been completely defined,[1a,35] especially when the counteranion is included. In principle, either olefin coordination[4f] (Figure 5a) or insertion (Figure 5b) could be rate-limiting.[1a−c] Quantum chemical analyses[35] at several levels argue that olefin coordination is exothermic for the naked cations (∼20 kcal/mol), subsequent insertion proceeds with little or no barrier (∼0−7 kcal/mol), and it is highly exothermic. Addition of the counteranion complicates this picture; however, it seems reasonable that olefin activation would be more anion-sensitive than insertion. Surprisingly little experimental activation energetic data relating to these reaction coordinates is available, with $E_a \sim 14$ kcal/mol for $(Me_4Cp)SiMe_2(N^tBu)TiCl_2$/MAO-mediated ethylene−styrene copolymerization[36a] and ∼7 kcal/mol for $(neomenthylC_5H_4)_2ZrCl_2$/MAO-mediated ethylene polymerization.[36b] Preliminary efforts in this laboratory[37] to estimate ethylene polymerization activation energetics for various zir-

(33) Chen, Y.-X., Marks, T. J. Manuscript in preparation.
(34) Bovey, F. A. *Chain Structure and Conformation of Macromolecules*; Academic: New York, 1982; pp 78−91.
(35) For relevant theoretical studies see: (a) Lohrenz, J. C. W.; Woo, T. K.; Fan, L.; Ziegler, T. *J. Organomet. Chem.* **1995**, *497*, 91−104. (b) Yoshida, T.; Koga, N.; Morokuma, K. *Organometallics* **1995**, *114*, 746−758. (c) Bierwagen, E. P.; Bercaw, J. E.; Goddard, W. A., III. *J. Am. Chem. Soc.* **1994**, *116*, 1481−1489. (d) Woo, T. K.; Fan, L.; Ziegler, T. *Organometallics* **1994**, *13*, 432−433. (e) Weiss, H.; Ehrig, M.; Ahlrichs, R. *J. Am. Chem. Soc.* **1994**, *116*, 4919−4928. (f) Castonguay, L. A.; Rappe, A. K. *J. Am. Chem. Soc.* **1992**, *114*, 5832−5842.
(36) (a) Sernetz, F. G.; Mülhaupt, R.; Waymouth, R. M. *Macromol. Chem. Phys.* **1996**, *197*, 1071−1083. (b) Chien, J. C. W.; Razavi, A. *J. Polym. Sci., Part A: Polym. Chem.* **1988**, *26*, 2369−2380.
(37) Ishihara, A.; Jia, L.; Marks, T. J. Manuscript in preparation.

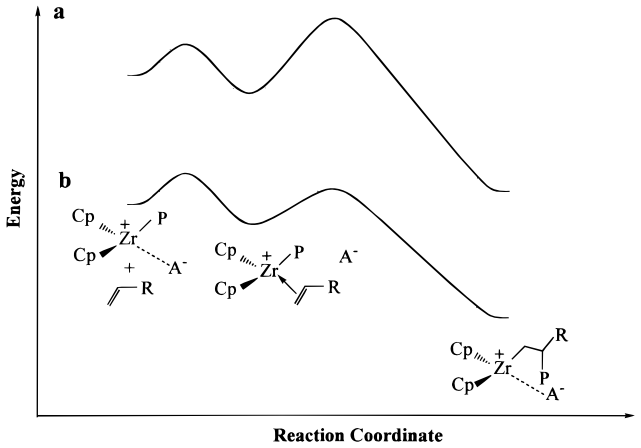

Figure 5. Plausible energetic profiles for olefin activation and insertion at metallocenium ion pairs.

Scheme 2

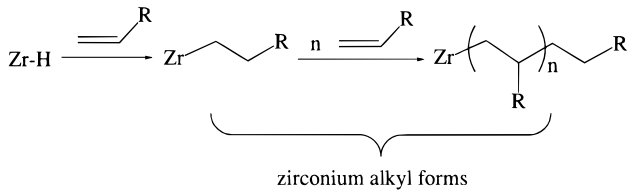

conocenes paired with $MeB(C_6F_5)_3^-$ *vs* $B(C_6F_4TBS)_4^-$ reveal $\Delta H^{\ddagger} \approx 2-10$ kcal/mol, with the former anion exhibiting the greatest cation sensitivity (~10 kcal/mol for Cp_2ZrR^+ *vs* ~2 kcal/mol for $(Me_5Cp)_2ZrR^+$), while results with the latter anion are more monotonic (~4 kcal/mol for Cp_2ZrR^+ *vs* ~7 kcal/mol for $(Me_5Cp)_2ZrR^+$). Importantly, if ion-pair reorganization processes such as those in eqs 8 and 10 represent the extreme in the energetic requirements for ion-pair separation (19−24 kcal/mol; Table 3) then either this degree of dissociation is not required for olefin activation (since $\Delta H^{\ddagger}_{\text{polymerization}} < \Delta H^{\ddagger}_{\text{eq 8,10}}$) or the energetic demands of ion pair dissociation are smaller when the σ-alkyl group is a polymer chain and/or are partially compensated by concurrent olefin complex formation (Figure 5b) or insertion (Figure 5a) in a concerted transition state.

IV. Further Discussion. Catalyst Thermal Stability and Activity. For efficient catalytic processes, the ideal situation is that the catalyst be both highly active and thermally stable. It is therefore important to understand how these two properties are related. Since the present catalysts arguably exist in a metal alkyl form at most stages in the catalytic cycle (Scheme 2), the stability of the metal alkyls is of greater interest than that of the corresponding hydrides. Metal methyl compounds can be regarded as working models of alkyls. As discussed previously, the thermal decomposition of the ion-paired methylzirconium complexes can be classified as follows: (i) decomposition involving the counteranion or (ii) cation self-decomposition. The first decomposition mode can be retarded or even prevented by either exogenous Lewis base coordination, which is not desirable because it will suppress catalytic activity,[1,2] or by using robust anions. As an example, the stability of the $(1,2\text{-}Me_2Cp)_2ZrMe^+$ system improves significantly when protected $B(C_6F_4TBS)_4^-$ and $B(C_6F_4TIPS)_4^-$ are used as charge-compensating anions instead of $MeB(C_6F_5)_3^-$. However, no obvious stabilization of the Cp_2ZrMe^+ system is observed and still more robust anions are required in this case. The second type of decomposition channel appears to be blocked only by employing strongly coordinating Lewis bases, such as the counteranions. However, as noted above, Lewis base coordination also suppresses catalytic activity. Therefore, anion Lewis basicity properties must be balanced sterically and electronically with cation Lewis acidity properties to obtain ion-paired catalysts with optimal stability and activity. One example of a catalyst which may be nearer optimal is $(1,2\text{-}Me_2Cp)_2Zr\text{-}Me^+B(C_6F_4TBS)_4^-$, which has both good thermal stability and polymerization catalytic activity. The $B(C_6F_5)_4^-$-based systems are representative examples of catalysts in which the anion coordination is apparently too weak to stabilize the highly electrophilic cations. Of course, these correlations are presently empirical, and further cation−anion pair elaboration and characterization is needed to better define the boundary conditions.

Conclusions

Two silyl-functionalized/protected derivatives of the tetrakis(perfluoroaryl)borate anion, $B(C_6F_4TBS)_4^-$ and $B(C_6F_4TIPS)_4^-$ (TBS = *tert*-butyldimethylsilyl and TIPS = triisopropylsilyl) have been synthesized, and a series of stable, highly reactive Zr and Th ion-paired methyl and hydride catalysts have been isolated using these anions. In contrast, the analogous $B(C_6F_5)_4^-$-based zirconocene methyl complexes are not stable at room temperature; however, $B(C_6F_5)_4^-$-based zirconocene hydride complexes can be isolated. The relative coordinative ability of the series of fluoroarylborates with respect to metallocene cations has been evaluated on the basis of spectroscopic and reactivity data and follows the approximate order $MeB(C_6F_5)_3^- > B(C_6F_4TBS)_4^- \approx B(C_6F_4TIPS)_4^- > B(C_6F_5)_4^-$. In cases of weakly coordinatiing anions, the neutral metallocenes compete with the anions for the cationic metallocenes, forming dimeric μ-Me complexes. Arene solvent coordination to the constrained geometry cation $[(Me_4Cp)SiMe_2(N^tBu)]\text{-}ZrMe^+$ is observed only when weakly coordinating $B(C_6F_5)_4^-$ is the counterion. The thermal stabilities of the $B(C_6F_4TBS)_4^-$- and $B(C_6F_4TIPS)_4^-$-based complexes have been studied and are found to be generally greater than those of the $MeB(C_6F_5)_3^-$ analogues. The polymerization activity of the zirconocene catalysts reaches a maximum when $B(C_6F_4TBS)_4^-$ and $B(C_6F_4TIPS)_4^-$ are counteranions, and the polymerization activity of the Zr constrained geometry catalyst reaches a maximum in aromatic solvents due to arene coordination when $B(C_6F_5)_4^-$ is the counteranion.

Acknowledgment. This research was supported by the U.S. Department of Energy (Grant DE-FG02-86ER13511). L.J. thanks Akzo-Nobel Chemicals for a predoctoral fellowship. We thank Dr. D. A. Kershner of Akzo-Nobel for GPC analyses.

Supporting Information Available: Complete X-ray experimental details and tables of bond lengths, angles, and positional parameters for the crystal structures of **8c** and **11** (50 pages). Ordering information is available on any current masthead page.

OM960880J